TEMPERATURE ANALYSIS OF COOLED GAS TURBINE BLADES UNDER TRANSIENT CONDITIONS

by

ABDULLAH ÖNGÖREN

B.S. in M.E., Boğaziçi University, 1978

Submitted to the Faculty of Engineering
in partial fulfillment of
the requirements for the degree of
Master of Science
in
Mechanical Engineering

Boğaziçi University

1981

APPROVED BY :

Prof. Dr. AKIN TEZEL .....

Doç. Dr. FAHİR BORAK .....

Dr. TANER DERBENTLİ .....
(Thesis Supervisor)

DATE :

28.8.1981

ACKNOWLEDGEMENT

I am indebted to my supervisor Dr. Taner Derbentli, B.Ü. Assistant Professor, for his continuous support and encouragement during this study. I received invaluable suggestions, comments and criticisms from him.

I wish to express my appreciation to my previous supervisor Dr. Ahmet Rasim Büyüktür, B.Ü. Professor, for helping me to start this study and for his valuable discussions afterwards.

My thanks are also due to the jury members of this thesis, Dr. Akın Tezel, B.Ü. Professor, and Dr. Fahir Borak, B.Ü. Associate Professor, for their help and comments about the presentation of the material.

TABLE OF CONTENTS

SUMMARY

In this thesis transient temperature and stress distributions in turbine blades were investigated numerically,Finite element method was used as the numerical technique to calculate the temperature fields in three gas turbine rotor blades having different cooling effectivenesses but the same external geometry.The transient temperature distributions at three locations where transient effect is significant were given,Also the isoterm contours at three different times in the transition period were contained.In order to examine the effect of transient temperature distributions on blade life thermal stresses were calculated by using a finite difference scheme applied to thermoelasticity.Close relations between cooling geometry and magnitude of thermal stresses were observed.Besides overall cooling effectiveness,local cooling effectiveness is also an important parameter.Even if most of the blade is effectively cooled,existance of less cooled parts causes problems by giving rise to high temperature differences in the blade and so, creating high thermal stresses.

During start and shut-down operations of gas turbines transient temperature distributions become very complicated.In these periods temperature gradients are very high both in chordwise direction and between the skin and core region of a blade.Because of these high gradients,magnitudes of thermal stresses in blades are also very high in these periods.

ÖZET

Bu tezde türbin kanatlarındaki geçici sıcaklık ve gerilim dağılımları sayısal olarak incelenmiştir. Dış geometrileri aynı olan fakat değişik soğutma etkinliklerine sahip üç gaz türbini rotor kanadındaki sıcaklık alanlarının hesaplanmasında sonlu elemanlar sayısal yöntemi kullanılmıştır. Geçicilik etkisinin belirgin olduğu üç bölgede geçici sıcaklık dağılımları verilmiştir. Tez aynı zamanda geçicilik süreci içindeki üç değişik zamana ait eşsıcaklık eğrilerini içermektedir. Geçici sıcaklık dağılımlarının kanat ömrü üzerine etkisini incelemek için ısısal gerilim dağılımları hesabedilmiş, bunun için ise sonlu farklar yöntemi kullanılmıştır.

Soğutma kanal geometrisi ve ısısal gerilim şiddetleri arasında yakın ilişkiler görülmektedir. Toplam soğutma etkinliğinin yanısıra, yerel soğutma etkinliği de önemli bir parametredir. Bir kanadın büyük bölümü iyi bir şekilde soğutulsa bile, az soğutulmuş bölgelerin varlığı büyük sıcaklık farklılıklarına yol açmakta ve böylece yüksek ısısal gerilimler yaratmaktadırlar.

Gaz türbinlerini çalıştırma ve durdurma işlemleri sırasında geçici sıcaklık dağılımları çok karmaşık bir hal almaktadır. Bu sırada sıcaklık gradyanı hem kanat boyunca hem de enlemesine çok büyüktür. Bu süreçte, böyle büyük gradyanların oluşması nedeniyle ısısal gerilim şiddetleri de çok büyük olmaktadır.

NOMENCLATURE

A	Conduction matrix, arbitrary region, area
C	Capacitance matrix
D	Arbitrary domain
E	Modulus of elasticity
F	Thermal force vector, transformed mapping function
I	Arbitrary subdomain
J	Jacobian matrix, arbitrary subdomain
N	Shape function
P,R	Weight coefficient
S	Surface boundary, perimeter
T	Temperature field variable
Z	Shape factor for cooled blades
a	Arbitrary constant
a,b,c	Local strains
a...h	Coordinates of integration points
c	Heat capacity
f	Mapping function, arbitrary function
h	Convective heat transfer coefficient
k	Thermal conductivity
l	Chord length, length of a line segment
m	Number of elements
n	Number of nodal points, outward normal vector
p,r	Number of integration points
s	Peripheral length

t time variable

x,y Global coordinates

det Determinant

α Coefficient of linear expansion, arbitrary constant

ϵ Strain

λ Arbitrary constant

ρ Density

σ Stress

ξ, η Local coordinates

SUBSCRIPTS

B Prescribed values at the boundary

c Cooling passage

i,j Node numbers

x,y Variables in x and y directions

0 Initial value

1...8 Local node numbers

1...n Global node numbers

∞ External condition

SUPERSCRIPTS

T Transpose

e Elemental value

-1 Inverse

* Average value

LIST OF FIGURES

I. INTRODUCTION

Today, the continious increase in the costs of fuel has made the high specific power and the high thermal efficiency an essential requirement in the design of gas turbines. But these two parameters mean high turbine inlet temperature as it has been investigated and confirmed by many researchers. They are functions of turbine inlet temperature and both specific power and thermal efficiency increase with increasing inlet temperature.

However, the inlet temperature is limited by the restrictions in the ultimate strengths and melting points of existing materials used in the production of gas turbine components. The cooling of the turbine blades is among the solutions of the problem. At present approximately 1100 °C maximum inlet temperature has been reached with the cooled blades in gas turbines, [1].

On the other hand, besides the afore-mentioned advantages of high working temperature in gas turbines, the long time rupture and corrosion behaviour of the heat resistant materials depend mainly on temperature. Especially the start-shut down operations or load fluctuations of turbines create transient temperature distributions in turbine blades and thereon cyclic thermal stresses appear which cause failure due to low cycle fatigue in the blades.

Hence, the investigation of gas turbine blades under transient conditions has a two fold importance and the analysis of results should

be made with care since it will provide the way of optimizing the maximum working temperature of the gas turbines.

In the design of a gas turbine, the life estimation of blades includes an important part of the work. Given the shape of blades and cooling geometry, the external and internal flow ratios and the heat transfer coefficients on the blade surfaces are determined both analytically and experimentally. Thenon, the results obtained are used as the means to determine the temperature and the stress distributions in the blade sections. The tool to compute the steady-state or the transient distributon of temperature and accordingly the stress is generally the numerical analysis with various computer programs. The insight offered by these calculations enables us to determine the permissable number of cycles that the blades can withstand.

The finite element is one of the numerical analysis techniques that can be used for above mentioned calculations. This method is adequate especially for the problems whose solution domains have irregular geometries. In this thesis, the gas turbine blades with their complex geometries are thought to be discretisized best with the finite elements. So, the finite element method is applied to the problem to obtain the temperature distributions in the blades. The superiority of the finite element method in the steady-state problems is put forward by Emery and Carson, [2]. Hence, by taking this fact into consideration, in this study the spacewise solution of the unsteady problem is obtained by this method.

On the other hand, in the solution of the remaining time dependent ordinary differantial equation, Euler method has been utilized. This method is examined to be the most accurate method in time marching problems again by Emery and Carson, [2]. This combined method is thought to be the most convenient one in solving the governing unsteady equation of the thesis.

In the finite element formulation of the differential equation, the method of Galerkin has been used. In such formulations, generally the classical variational method is used. But this method is not applicable to parabolic type of equations, likewise the case in this thesis. In such cases, a quasi-variational method can be utilized as has been proposed by Gurtin, [3]. In fact, the functional obtained

by Galerkin method is just the same as the one obtained by the quasi-variational method, [4].

The boundary conditions on both the outer surfaces and the inner surfaces have been assumed to be purely convective. In reality, this is not the case, of course, and especially the effect of radiation heat transfer can not be neglected. But, when the heat flux emmited by radiation onto the blade is considered and applied to the proble the boundary conditions become non-linear. It is hard to solve the problem in this complicated form. This is the reason for taking the boundary conditions to be purely convective. But, besides, in this thesis, a convective heat transfer coefficient, h, which is corrected for the effect of radiation has been used, [5]. This application compensates the error that results from neglecting the radiation term in the governing differential equation.

The external gas temperature is 1145 °C. This temperature resembles both the highest temperature that a blade material can withstand [1], and the temperature giving the highest performance. In a way this temperature is the extreme test temperature by which it can be obtained the severest conditions that may occur in a blade.

The thermal analysis of the cooled gas turbine blades is undertaken as a two-dimensional transient problem. Thus, the governing equation of the problem is two-dimensional transient heat conduction equation. The three-dimensional thermal analysis of gas turbine blades under steady-state conditions has been carried out by Camci [6] and the thermal fields determined for various blade geometries have been given. The investigation of these fieldsshows that neglecting the radial temperature distribution does not give rise to serious errors whereas, it simplifies the problem very much. The temperature gradient in radial direction is low enough to neglect.

In a transient problem, the time range is also an important parameter. The investigations have shown that twenty four seconds is the period to reach the steady-state conditions for all three blades used in this thesis. So, the analysis has been carried out in this period. As the time increment, Δt, of Euler method becomes small, the results converge to the exact solution. Therefore, the minimum time increment allowed by the CPU time of the computer used has been

selected, Namely, this value is sixty milliseconds. In fact, the order of magnitude of the error due to Euler method of integration is proportional to the square of the time increment. Thus, in this particular case the error due to numerical time integration is less than one percent.

Besides the thermal fields, the analysis of thermal stresses caused by these thermal fields are also included in the thesis. The determination of thermal stresses has been made by using finite difference method which is investigated and proposed by Mukherjee, [7] and Barnes and Fray, [8].

II. LITERATURE SURVEY

The cooling of turbine blades is one of the most important research areas in todays gas turbine technology, since it is the most applicable mean to increase thermal efficiency and specific power. In order to achieve the most effective cooling many types of cooled blades have been designed up to now, Convection, film, transpiration, thermosyphon, and impingement cooling are the most utilized blade cooling methods and they are explained in detail in reference [9] and [6], A study on the cooling of gas turbine blades which contains the investigation of cooling effect on blade life has been published by Mukherjee, [1], in 1977. Besides cooling studies, there are many studies investigating heat transfer mechanisms on turbine blades but the work done by Mukherjee and Frei, [10], in 1974 in which they measured temperature distributions on two first-stage air-cooled vanes of a gas turbine during the test run, the study done by Consigny et al., [11], in 1979 in which they obtained the heat trasfer rate distributions on a turbine blade as affected by inlet Mach number and free stream turbulance level and a recent study done by Graziani et al., [12], in 1980 upon the heat transfer distribution on the blades in the vicinity of secondary flows have particular importances as the subject of this thesis is concerned. The study containing experimental results of the cooling performance of various convection and film cooled turbine blade models in a two-dimensional stationary cascade done by Hennecke et al., [5], should also be mentioned.

The cooling of blade and heat transfer on blades studies are always considered together in order to achieve the most effective cooling geometry.In such cases the heat transfer in the blade itself should be known.In past,to solve the heat transfer in blades,many analytical methods have been applied which approximate the blade as a simple geometrical domain.The studies established by Pollmann, [13] in 1947 and Panteleev and.Trushin, [14] ,in 1974 are examples to such approaches,But today such methods are not used anymore and some numerical methods which approximate blades much more accurately are studied,Finite element method is one of these numerical approaches.

Although it is a new approach,in solving the problems governed by differential equations,there are numerous publications about finite element method in the literature,After introduced by Zienkiewicz [15,16] ,this method became quite popular and attempt has been made to apply it to almost all fields of engineering.A detailed survey of finite element method is given by Huebner, [4] .An application of finite element method to heat conduction problems is given by Wilson and Nickel, [17] ,in 1966 and this study has been used as a reference in almost all studies done after 1966 in this field.In their study,Wilson and Nickel have made the transient heat conduction analysis of complex solids of arbitrary shape with temperature and heat flux boundary conditions by finite element method utilizing a variational principle.In this study authors discuss also various shapes and their associated temperature fields for one,two and three-dimensional bodies by systems of simplex elements.In 1970, Zienkiewicz and Parekh, [18] ,have formulated the transient field problems of the type encountered in heat conduction problems in terms of finite element process using Galerkin approach in a generalized manner,Curved two-dimensional and three-dimensional isoparametric elements have been used in a time stepping solution and various examples are given to illustrate the applicability of this procedure.Following this study,Emery and Carson, [2] ,have discussed the use of finite element method in the computation of temperature in 1971.They investigated accuracy and efficiency of the finite element method in comparison with the standard finite difference algorithms used for the computation of temperature.Again in 1971, Gallager and Mallet, [19] ,have presented systematic procedures for reducing the order of a matrix differential equation governing

transient heat conduction in solids.Two-dimensional transient heat conduction problem has been solved for various domains and results have been compared with the analytical solutions by both Bruch and Zyvaloski, [20] and Köhler and Pittr, [21] , in 1974.Köhler and Pittr have applied finite element method also to the time domain.

The application of finite element method to solve heat transfer in blades is given by Hogge, [22] ,in 1976.In his study the author presented the main approaches to calculate thermal fields and stresses in cooled turbine blades using so-called temperature and displacement models and considering all kinds of heat transfer,even the non-linear case.Various situations concerning turbine blades are analyzed.In 1979,Camcı, [6] , used the same method to solve turbine blade heat transfer but in this study he has taken the problem as steady-state and three-dimensional problem .He has investigated various blades under favorable gas turbine conditions.

III. THEORY

3.1. TWO-DIMENTIONAL TRANSIENT HEAT CONDUCTION PROBLEM

The two-dimentional transient heat conduction problem is governed by the following differential equation in the domain, D,

$$\frac{\partial}{\partial x}\left(k_x \frac{\partial T}{\partial x}\right)+\frac{\partial}{\partial y}\left(k_y \frac{\partial T}{\partial y}\right)=\varrho c \frac{\partial T}{\partial t} \tag{1}$$

subjected to the conditions on the boundary, S,

$$T=T_B \quad \text{on} \quad S_1 \quad \text{at} \quad t>0 \tag{2}$$

$$k_x \frac{\partial T}{\partial x} n_x + k_y \frac{\partial T}{\partial y} n_y + h(T-T_\infty)=0 \quad \text{on} \quad S_2 \quad \text{at} \quad t>0 \tag{3}$$

and the initial condition,

$$T=T_0 \quad \text{at} \quad t=0 \tag{4}$$

where:
$T(x,y,t)$ is the temperature,
k_y, k_x are thermal conductivities in the x and y-directions,
ϱ is the density,
c is the specific heat capacity of the solid,
h is the convective heat transfer coefficient,
T_o is the ambient temperature, and
n_x, n_y are the direction cosines of the outward normal vector n to the boundary, S.

3.2. FINITE ELEMENT FORMULATION BY GALERKIN METHOD

The process by which one might deduce the discretization of the differential equation (1) begins with the assumption that the unknown exact solution $T(x,y,t)$ may be approximated, element by element, as,

$$T^{(e)}(x,y,t) \approx \sum_{i=1}^{n} N_i(x,y)\, T_i(t) = \left[N_1, N_2, \ldots\ldots, N_n\right]\left\{T\right\}^{(e)} \qquad (5)$$

where N_i are the assumed shape functions and T_i are the unknown nodal values of $T(x,y,t)$, The alternate variational expression of equation (1) is obtained by Galerkin method, The application of Galerkin method to the differential equation (1) yields,

$$\int_{D^{(e)}} N_j \left\{ \left[\frac{\partial}{\partial x}\left(k_x \frac{\partial}{\partial x}\right) + \frac{\partial}{\partial y}\left(k_y \frac{\partial}{\partial y}\right) \right] \sum_{i=1}^{n} N_i T_i - \varrho c \frac{\partial}{\partial t} \sum_{i=1}^{n} N_i T_i \right\} dx\, dy = 0 \qquad (6)$$

$$j = 1, 2, \ldots\ldots, n$$

Integration by parts can be applied to equation (6) in order to simplify it, The simplified form of (6) is,

$$-\int_{D^{(e)}} \left(k_x \frac{\partial N_j}{\partial x}\frac{\partial T}{\partial x} + k_y \frac{\partial N_j}{\partial y}\frac{\partial T}{\partial y} + N_j \varrho c \frac{\partial T}{\partial t} \right) dx\, dy - \int_{S_1} N_j h\,(T - T_\infty)\, dS_1 = 0 \qquad (7)$$

Now, inserting the approximate form of the unknown variable, $T(x,y,t)$ given by equation (5) into equation (7), one obtains,

$$-\int_{D^{(e)}} \left(k_x \frac{\partial N_j}{\partial x} \sum_{i=1}^{n} \frac{\partial N_i}{\partial x} + k_y \frac{\partial N_j}{\partial y} \sum_{i=1}^{n} \frac{\partial N_i}{\partial y} \right) T_i \, dx\, dy$$

$$-\int_{D^{(e)}} N_j \, \varrho c \left(\sum_{i=1}^{n} N_i \frac{\partial T_i}{\partial t} \right) dx\, dy + \int_{S_1} N_j \left(k_x \sum_{i=1}^{n} \frac{\partial N_i}{\partial x} n_x \right. \qquad (8)$$

$$\left. + k_y \sum_{i=1}^{n} \frac{\partial N_i}{\partial y} n_x \right) T_i \, dS_1 = 0$$

The system resulting from equation (8) will consist of n linear algebraic equations in n unknowns, Evaluation of the integrals in equation (8) will allow the complete solution of the problem. n such equations appearing in equation (8) can be put into a matrix form as,

$$[C]^{(e)} \frac{\partial \{T\}^{(e)}}{\partial t} + [A]^{(e)} \{T\}^{(e)} + \{F\}^{(e)} = 0 \qquad (9)$$

where $[C]^{(e)}$, $[A]^{(e)}$ and $\{F\}^{(e)}$ are element capacitance matrix, element conduction matrix and element thermal force vector, respectively, and their contributions are,

$$[C]^{(e)} = \int_{D^{(e)}} \varrho c\, N_i\, N_j \, dx\, dy \tag{10}$$

$$[A]^{(e)} = \int_{D^{(e)}} \left(k_x \frac{\partial N_i}{\partial x} \frac{\partial N_j}{\partial x} + k_y \frac{\partial N_i}{\partial y} \frac{\partial N_j}{\partial y} \right) dx\, dy + \int_{S_1} h N_i N_j \, dS_1 \tag{11}$$

$$[F]^{(e)} = \int_{S_1} -h T_\infty N_j \, dS_1 \tag{12}$$

The global form of equations defining the whole solution domain will be obtained by the assembly of the element equations. Thus for the whole region it is obtained that,

$$[C] = \sum_{e=1}^{m} [C]^{(e)}$$

$$[A] = \sum_{e=1}^{m} [A]^{(e)} \tag{13}$$

$$\{F\} = \sum_{e=1}^{m} [F]^{(e)}$$

where m is the number of elements and $[C]$, $[A]$ and $\{F\}$ are global capacitance matrix, global conduction matrix and global thermal force vector, respectively. Hence the resultant system of equations may be expressed as,

$$[C] \frac{\partial \{T\}}{\partial t} + [A] \{T\} + \{F\} = 0 \tag{14}$$

3.3. DISCRETIZATION OF SOLUTION DOMAIN

The finite element method divides the solution domain into sub-domains called ELEMENTS and it defines local approximations to the governing equations each of which is valid for only one element. Finally, the assemblage of these discrete elements gives the approximated solution domain.

Even if curved boundaries of a domain can be represented satisfactorially by straight-sided elements, they are best fitted by curvilinear elements. Moreover, availability of such elements reduce the number of elements in a mesh by providing enlargement in element sizes without losing the close representation of boundaries. Therefore, in this thesis the gas turbine blades which were considered as the domains to the problem described in section 4,1 have been discretisized into curvilinear elements. The finite element meshes of the considered blades are given in Fig.11, Fig.12 and Fig.13.

Assignment of the nodal points or in other words, selection of degree of shape functions mainly depends on the accuracy needed in the solution. As has been investigated by Emery and Carson, [2], the computation of temperature in the two-dimensional transient heat-conduction problem may be established best by "quadratic elements". Thus, quadratic approximation which is shown in Fig.2 has been preferred in this study.

3.4. VARIATION OF TEMPERATURES IN ELEMENTS

The behaviour of a field variable in an element can be represented by the functions which are called SHAPE FUNCTIONS in the finite element terminology. Many types of functions can be used as shape functions among which are the polynomials and the trigonometric functions, but a few are easy to treat. The polynomials are the most appropriate tools providing an easy and systematic method of generating shape functions of any order.

If a rectangular element with eight nodes shown in Fig.3 is considered, the variation of the field variable T(x,y,t) is quadratic in both ξ and η-directions.Thereof this element is called QUADRATIC and the variation of field variable may be expressed as,

$$T(\xi,\eta) = T_1 N_1 + T_2 N_2 + \cdots\cdots + T_8 N_8 = \sum_{i=1}^{8} N_i(\xi,\eta)\, T_i \qquad (15)$$

where N_i's are the easily generated quadratic polynomials defined in ξ and η coordinates and T_i's are the unknown nodal values of the field variable T(x,y,t).The shape functions of rectangular quadratic element are given in Appendix A.The derivation of the shape functions and the particular shape functions for other types of elements can be found in Zwienkiewicz, [15] ,Ergatouidis et al., [23] and Huebner, [4] ,in detail.

3,5. ISOPARAMETRIC TRANSFORMATION

Since the domain of the problem investigated is not discretisized into rectangular elements but into curvilinear elements in the global Cartesian coordinate system,it is not possible to use the simple shape functions defined above,directly in these elements to interpolate the field varible.But if it is possible to establish a transformation between the rectangular element of Fig.3 into the distorted elements of Fig.2,then the resulting element equations for the curve-sided elements can be evaluated.

The coordinate transformation from local to global as shown in Fig.4 can be achieved by expressions similar to equation (15) as,

$$x = \sum_{i=1}^{8} f_i(\xi,\eta)\, x_i \qquad (16)$$

$$y = \sum_{i=1}^{8} f_i(\xi, \eta)\, y_i \qquad (17)$$

In order to map the nodes of quadratic element into distorted global element of turbine blade, the mapping functions should also be quadratic and at the same time the evaluation of the expressions (16) and (17) at any node should result in the value of that node. A group of functions meeting above requirements are the shape functions of quadratic elements used to interpolate the unknown field variable. This means that,

$$f_i(\xi, \eta) = N_i(\xi, \eta) \qquad (18)$$

and consequently it is possible to write,

$$x = \sum_{i=1}^{8} N_i(\xi, \eta)\, x_i \qquad (19)$$

$$y = \sum_{i=1}^{8} N_i(\xi, \eta)\, y_i \qquad (20)$$

Curve-sided elements whose geometry are defined by the shape functions interpolating the field variable are called ISOPARAMETRIC.

3.6. COORDINATE TRANSFORMATION IN ELEMENT MATRICES

When the element equation of the problem given as equation (8) is investigated, it is seen that the terms of matrices are in general integrals of the form,

$$\int_{D^{(e)}} f\left(N_i, \frac{\partial N_i}{\partial x} \quad \frac{\partial N_i}{\partial y}\right) dx\, dy \tag{21}$$

where $D^{(e)}$ is the area of the curve-sided element, As mentioned earlier N_i are functions of the local coordinates ξ and η and therefore it is necessary to express $\partial N_i/\partial x, \partial N_i/\partial y$ and $dx dy$ in terms of ξ and η.

Considering equations (19) and (20) and applying the chain rule of differentiation, it can be written that,

$$\frac{\partial N_i}{\partial \xi} = \frac{\partial N_i}{\partial x}\frac{\partial x}{\partial \xi} + \frac{\partial N_i}{\partial y}\frac{\partial y}{\partial \xi} \tag{22}$$

$$\frac{\partial N_i}{\partial \eta} = \frac{\partial N_i}{\partial x}\frac{\partial x}{\partial \eta} + \frac{\partial N_i}{\partial y}\frac{\partial y}{\partial \eta} \tag{23}$$

or in a more compact form,

$$\begin{Bmatrix} \frac{\partial N_i}{\partial \xi} \\ \frac{\partial N_i}{\partial \eta} \end{Bmatrix} = \begin{bmatrix} \frac{\partial x}{\partial \xi} & \frac{\partial y}{\partial \xi} \\ \frac{\partial x}{\partial \eta} & \frac{\partial y}{\partial \eta} \end{bmatrix} \begin{Bmatrix} \frac{\partial N_i}{\partial x} \\ \frac{\partial N_i}{\partial y} \end{Bmatrix} = [J] \begin{Bmatrix} \frac{\partial N_i}{\partial x} \\ \frac{\partial N_i}{\partial y} \end{Bmatrix} \tag{24}$$

where $[J]$ is known as Jacobian matrix, To find the required global derivatives of N_i, equation (24) is inverted as,

$$\begin{Bmatrix} \frac{\partial N_i}{\partial x} \\ \frac{\partial N_i}{\partial y} \end{Bmatrix} = [J]^{(-1)} \begin{Bmatrix} \frac{\partial N_i}{\partial \xi} \\ \frac{\partial N_i}{\partial \eta} \end{Bmatrix} \tag{25}$$

Similarly,the area element can be expressed as,

$$dx\,dy = \det\left[J\right]\, d\xi\, d\eta \tag{26}$$

Now,using equations (19) and (20) in equation (21),it can be formed integrals of the form,

$$\int_{-1}^{1}\int_{-1}^{1} F(\xi,\eta)\ \det\left[J\right]\, d\xi\, d\eta \tag{27}$$

as the terms of governing element equation (9).F is the transformed function of f in the above integral.

In the mean time,application of above procedure requires the existance of the inverse of J matrix for each element.This,at the same time,means that the coordinate mapping from local to global is unique.This fact should be checked strictly in the analysis of above kind.Otherwise a mathematically acceptible transformation is not possible.

As the result of substitutions given in equations (25) and (26), the element equations (10) and (11) become,

$$\left[C\right]^{(e)} = \int_{-1}^{1}\int_{-1}^{1} \varrho c\, N_i\, N_j\, \det\left[J\right]\, d\xi\, d\eta \tag{28}$$

$$\left[A\right]^{(e)} = \int_{-1}^{1}\int_{-1}^{1} k \begin{Bmatrix} \frac{\partial N_j}{\partial \xi} \\ \frac{\partial N_j}{\partial \eta} \end{Bmatrix} \left[J\right]^{(-1)T} \left[J\right]^{(-1)} \begin{Bmatrix} \frac{\partial N_i}{\partial \xi} \\ \frac{\partial N_i}{\partial \eta} \end{Bmatrix} \det\left[J\right] d\xi\, d\eta + \int_{S_1} h N_i N_j\, dS_1 \tag{29}$$

3.7. INTEGRATION TECHNIQUES

Even though the transformations performed provide simple integration limits,the transformed function F is generally not a simple

integrand that permits closed-form integration. Therefore, numerical integration is utilized in such cases. In this thesis also, the numerical integration is used.

When the finite element formulation of two-dimensional transient heat conduction equation with convective (Neumann) type of boundary conditions is investigated, it is observed that surface integrals exist in the domain of space and line integrals appear on its boundaries. In the matrix form of the above formulation, surface integrals are elements of heat conduction and heat capacitance matrices and line integrals are elements of convection matrices.

In the finite element solution of the equations, the surface integrals are evaluated by numerical integration technique whereas the line integrals are tackled analytically in this thesis. Simpson's rule is utilized as the numerical integration technique. Simpson's rule is one of the simplest techniques to apply in this particular case. Two-dimensional Simpson's rule is a nine point approximation performed by the values of the integrand function at these points. But, in any case eight of these points are obtained to be used in the finite element analysis. So, only one additional point completes the data needed for Simpson's rule of integration. Futhermore, the integrations approximated by two-dimensional Simpson's rule converge to their exact values provided that the integrated differential terms are at most of second order, [24]. In our case, the highest order is two for the existing integral terms. So, by using Simpson's rule the additional error due to numerical integration is reduced to zero percent. All integrations in the analysis are carried out in the local coordinate system and then transformed into global.

The elements of heat conduction and heat capacitance matrices are approximated by two-dimensional Simpson's rule as mentioned before. In the local coordinate system, consider M as a region in two-dimensional Euclidian space with points (ξ, η). Let M be a region composed of two subregions I and J where both regions are in one-dimensional Euclidean space with points (ξ) and (η), respectively. Then, by taking

I and J as r and p-point rules of integration over I and J, respectively, it can be expressed that,

$$I = \sum_{i=1}^{r} R_i f(\xi_i) \simeq \int_I f(\xi)\, dI \qquad \xi_i \in I \tag{30}$$

$$J = \sum_{j=1}^{p} P_j f(\eta_j) \simeq \int_J f(\eta)\, dJ \qquad \eta_j \in J \tag{31}$$

Thereon, the product rule gives the result as,

$$A = I \times J = \sum_{i=1}^{r} \sum_{j=1}^{p} R_i P_j f(\xi_i, \eta_j) \simeq \iint_A f(\xi, \eta)\, dA \tag{32}$$

Returning now to the particular problem considered in the thesis the domains on which the integrations are carried out, are the finite elements in the local coordinates. In this case, $I \times J$ designates the rectangular region where,

$$a \leq \xi \leq b$$

$$c \leq \eta \leq d$$

Since the three-point rule of integration in both directions is the most convenient one together with quadratic element having eight nodes, consideration of the product of two three-point Simpson's rules yields,

$$\iint_A f(\xi,\eta)\, dA \simeq \frac{ef}{36}\Big\{ f(a,c) + f(a,d) + f(b,c) + f(b,d) + 4\Big[f(a,h) + f(g,c) + f(b,h) + f(g,d)\Big] + 16 f(g,h)\Big\} \tag{33}$$

where,

$$e = b - c$$

$$f = d - c$$

$$g = \frac{1}{2}(a+b) \qquad (34)$$

$$h = \frac{1}{2}(c+d)$$

More particularly, if M is the square region of any element used in the local coordinate system where,

$$-1 \leq \xi \leq 1$$

$$-1 \leq \eta \leq 1 \qquad (35)$$

Then,

$$e = 2$$

$$f = 2 \qquad (36)$$

$$g = h = 0$$

and,

$$\iint_A f(\xi,\eta)\, dA = \frac{1}{9}\Big\{ f(-1,-1) + f(-1,1) + f(1,-1) + f(1,1) + 4\Big[f(-1,0) + f(0,-1) + f(1,0) + f(0,1)\Big] + 16 f(0,0)\Big\} \qquad (37)$$

Equation (37) is the one used to approximate all integral terms existing in the heat capacitance and conduction matrices.

The line integrals that are introduced to handle the boundary conditions exist as the elements of convection matrix and thermal force vector in the governing matrix equation. To simplify the integration along the boundary, s has been used as the coordinate direction as shown in Fig. 5-a. As it can be observed in Fig. 5, in forming the element convection matrix and thermal force vector the integral limits become s_1 and s_3 for each element boundary.

On the other hand, the shape functions for such a curved element boundary can be obtained by using Lagrange interpolation functions for a quadratic element in one-dimensional form. Considering s as the variable and the terminology of Fig. 5-b, it can be written that,

$$N_1 = \frac{(s-s_2)(s-s_3)}{(s_1-s_2)(s_1-s_3)} = \frac{(s-s_2)(s-s_3)}{s_2 s_3} \tag{38}$$

$$N_2 = \frac{(s-s_1)(s-s_3)}{(s_2-s_1)(s_2-s_3)} = \frac{(s)(s-s_3)}{(s_2)(s_2-s_3)} \tag{39}$$

$$N_3 = \frac{(s-s_1)(s-s_2)}{(s_3-s_1)(s_3-s_2)} = \frac{(s)(s-s_2)}{(s_3)(s_3-s_2)} \tag{40}$$

Now it is convenient to investigate the terms of convection matrix and thermal force vector. As it is also given in Appendix B, all terms of both parts contain only shape functions as variables. Then insertion of equations (38), (39) and (40) into these terms forms line integrals that can be easily calculated analytically. The results of these calculations are also given in Appendix B in terms of lengths s_2 and s_3 whose definitions are given in Fig. 5-b but their values are unknown.

The second stage of the line integral evaluation contains the calculation of s_2 and s_3 values. But this operation give rise to a new problem to be tackled. Since the behaviour of boundaries of complex surfaces considered is not specified, it is not possible to calculate s_2 and s_3 values analytically and so the numerical approximation appears as the most probable estimation of these values. Therefore, in this thesis a numerical approximation technique which uses the finite element method as a tool has been devised for the calculation of these values.

According to the technique devised, all boundaries are assumed to be composed of isoparametric line elements in quadratic forms and the isoparametric transformation shown in Fig.6 is considered. The shape functions for such an element can again be obtained by utilizing Lagrange interpolation functions and in this particular case have the forms,

$$N_1 = (1/2)\ (\xi - 1) \tag{41}$$

$$N_2 = (1 - \xi)\ (1 + \xi) \tag{42}$$

$$N_3 = (1/2)\ (1 + \xi)\ \xi \tag{43}$$

As was explained in section 3.5, the global coordinates of any point on this line element can be obtained by the isoparametric transformation which is expressed as,

$$x = N_1 x_1 + N_2 x_2 + N_3 x_3 = \{N\}^T \{x_i\} \tag{44}$$

$$y = N_1 y_1 + N_2 y_2 + N_3 y_3 = \{N\}^T \{y_i\} \tag{45}$$

where x and y are the coordinates of any point and x_i and y_i are the coordinates of nodal points on the line element in global coordinates, respectively.

Now consider the approximation of line element by the combination of a group of line segments as shown in Fig.7. The lengths of line segments shown in Fig.7-b can be evaluated easily if the coordinates of points from one to five are known, and their summation

gives s_2 and s_3 values accurately,The coordinates of points 1,2 and 3 are known from finite element data,Only the coordinates of points 4 and 5 remain to be found,Thereon,equations (44) and (45) will be used for this purpose,Evaluation of equations (44) and (45) at points,

$$\S = -0.5$$

$$\S = 0.5$$

provides the particular equations that can be used in the calculation of the coordinates of points 4 and 5,For point 4 the expressions (44) and (45) becomes,

$$x_4 = 0.375\,x_1 + 0.750\,x_2 - 0.125\,x_3 \qquad (46)$$

$$y_4 = 0.375\,y_1 + 0.750\,y_2 - 0.125\,y_3 \qquad (47)$$

and for point 5 the equations are,

$$x_5 = -0.125\,x_1 + 0.750\,x_2 + 0.375\,x_3 \qquad (48)$$

$$y_5 = -0.125\,y_1 + 0.750\,y_2 + 0.375\,y_3 \qquad (49)$$

Then,the following relations can be written,

$$l_1 = \left[(x_4 - x_1)^2 + (y_4 - y_1)^2 \right]^{1/2} \tag{50}$$

$$l_2 = \left[(x_2 - x_4)^2 + (y_2 - y_4)^2 \right]^{1/2} \tag{51}$$

$$l_3 = \left[(x_5 - x_2)^2 + (y_5 - y_2)^2 \right]^{1/2} \tag{52}$$

$$l_4 = \left[(x_3 - x_5)^2 + (y_3 - y_5)^2 \right]^{1/2} \tag{53}$$

Hence, s_2 and s_3 values can be evaluated as,

$$s_2 = l_1 + l_2 \tag{54}$$

$$s_3 = l_1 + l_2 + l_3 + l_4 \tag{55}$$

Consequently, the substitution of s_2 and s_3 values into the expressions of the terms of convection matrix and thermal force vector calculated before and given in Appendix B gives the numerical values of these terms.

3.8. FORMATION OF GLOBAL SYSTEM

The assemblage of global matrices is based upon a simple summation procedure. Application of this procedure on conduction matrix $[A]$ and thermal force vector $\{F\}$ is given in Fig.8 schematically. According to this procedure, the local node numbers specifying the terms of element matrix are replaced by global node numbers and these

terms are added to the terms of the global matrix specified by these new numbers,As an example,the term a_{33} of the element conduction matrix given in Fig.8 is changed to a_{pp} and then added to the corresponding term of the global conduction matrix,A_{pp}.The procedure is the same for thermal force vector as can be seen in Fig.8..

In the formation of the global system, the assemblage of global matrices is followed by the boundary condition corrections.In this thesis,for the elements having convective type of boundary conditions this operation is not applied because the governing differential equations have been derived as to include such boundary conditions.The thermal force vector $\{F\}$ is composed of those terms. But if prescribed temperature (Dirichlet) type of boundary conditions are imposed on the elements,then the global matrices need to be corrected for the boundary nodes of those elements.The schematic explanation of this procedure is given in Fig.8..

In this procedure,first the column corresponding to the node that is selected to be corrected is carried to the right hand side of the global matrix equation by subtracting it from the right hand side vector,namely the thermal force vector.As an example,the column p in Fig.8 can be considered.Then its elements and the elements of the row which is the transpose of this column,for example row p in Fig.8 which is the transpose of column p, are equated to zero.The procedure is finalized by assigning a value of one to the element corresponding to the node with prescribed temperature,likewise the node pp in Fig.8,in the global matrix and by assigning a value of the prescribed temperature to the element of the thermal force vector corresponding to the corrected node.This procedure is repeated for all nodes on which prescribed temperature type of boundary conditions are imposed.

3.9. INTEGRATION IN TIME DOMAIN

Two of the many popular procedures for solving the linear differential equation (14) for T values are Euler method and the one

dimensional finite element method.In this thesis the former is used since it needs less programming work and it is as accurate as the latter, [25].

Assume that two points at times t_o and t_1 on a curve are given and the derivative at the point, $(t+\alpha\Delta t)$, is required where,

$$0 \leq \alpha \leq 1 \tag{56}$$

and,

$$\Delta t = t_1 - t_0 \tag{57}$$

as illustrated in Fig. 9 .

In this case the following assumptions are possible,

$$\frac{dT}{dt}(t+\alpha\Delta t) = \frac{T(t+\Delta t) - T(t)}{\Delta t} \tag{58}$$

and,

$$T(t+\alpha\Delta t) = (1-\alpha)\,T(t) + \alpha\,T(t+\Delta t) \tag{59}$$

Using equation (14) together with equations (58) and (59) ,at time $(t+\alpha\Delta t)$ it is obtained that,

$$\frac{C(t+\Delta t)}{a_o}\,T(t+a_1\Delta t) + A(t+\alpha\Delta t)\,T(t+\alpha\Delta t) = F(t+\Delta t) + \frac{C(t+\alpha\Delta t)}{a_o}\,T(t) \tag{60}$$

and also,

$$T(t+\Delta t) = \frac{T(t+a_1\Delta t)}{a_1} + \left(1-\frac{1}{a_1}\right) T(t) \qquad (61)$$

where,

$$\begin{aligned} a_o &= \Delta t \quad \text{and} \quad a_1 = 1 \qquad \text{for} \qquad \alpha = 0 \\ a_o &= \alpha \Delta t \quad \text{and} \quad a_1 = \alpha \qquad \text{for} \qquad \alpha \neq 0 \end{aligned} \qquad (62)$$

But on the other hand, since C, A and F are independent of time and if it is assigned the subscript 1 to the values obtained at time $(t+\Delta t)$ and the subscript 0 to the values obtained at time (t), the equations (60) and (61) can be obtained to form the equation,

$$\left(\frac{C}{\Delta t} + \alpha A\right)(T_1 - T_0) = F(t+\alpha\Delta t) - AT_0 \qquad (63)$$

This discretization formula is so-called Euler formula with time step $(\alpha\Delta t)$, A family can be formed by using Euler formula with different α values, In this family,

$\alpha = 0$	corresponds to the explicit Euler scheme
$\alpha = 1/2$	corresponds to the trapezoidal rule
$\alpha = 2/3$	corresponds to the Galerkin scheme
$\alpha = 1$	corresponds to the pure implicit Euler scheme

The selection of the value of α owes to the type of the problem considered, In the problems where short time accuracy is needed the Galerkin scheme may be used. If long time steps are required, the pure implicit Euler scheme and if long time solution is needed the trapezoidal rule may be used, [26].

For any linear relation, likewise the system of equations obtained in this thesis, in form,

$$\frac{dT}{dt} + \lambda T = 0 \tag{64}$$

where λ is a constant, the stability criteria is, [26],

$$\left| \frac{1 - (1 - \alpha)\Delta t \lambda}{1 + \alpha \lambda \Delta t} \right| \leq 1 \tag{65}$$

This expression leads to the following results:

a) for $\alpha \geq 1/2$ the scheme is unconditionally stable

b) for $\alpha < 1$ the scheme is stable provided that,

$$\Delta t \leq \frac{2}{\lambda(1 - 2\alpha)} \tag{66}$$

Using the trapezoidal rule to discretisize the time domain equation (60) takes the form,

$$\left(\frac{[C]}{\Delta t} + \frac{1}{2}[A] \right)\left(\{T_1\} - \{T_o\} \right) = \left\{ F(t + \frac{1}{2}\Delta t) \right\} - [A]\{T_o\} \tag{67}$$

which reduces to the collected form,

$$\left([A] + \frac{2}{\Delta t}[C] \right)\{T_1\} = \left(\frac{2}{\Delta t}[C] - [A] \right)\{T_o\} - 2\left\{ F(t + \frac{1}{2}\Delta t) \right\} \tag{68}$$

But if the following definition is used,

$$\{F^*\} = F(t + \tfrac{1}{2}\Delta t) = \tfrac{1}{2}(\{F_1\} + \{F_0\}) \tag{69}$$

the final form of governing equation becomes,

$$([A] + \tfrac{2}{\Delta t}[C])\{T_1\} = (\tfrac{2}{\Delta t}[C] - [A])\{T_o\} - 2\{F^*\} \tag{70}$$

IV. THERMAL STRESS ANALYSIS

4.1. THERMAL STRESS CALCULATIONS

When the temperature gradients in a body are high,then considerable thermal stresses appear in that body which are frequently an important factor in determining material life.In cooled gas turbine blades also,especially during start and shut-down operations,high temperature gradients exist on blade sections.This fact may be observed in section VI of this thesis and in Fig.16,17 and 18. Hence,thermal stress analysis becomes an unavoidable matter.

Both analytical and numerical methods canbe used to predict thermal stress distributions in an elastic body with the temperature distributions given.The various aspects of analytical methods are discussed in Boley et al,[27] and Gatewood,[28] ,There are also many numerical approaches applied to thermal stress calculations one of which is investigated by Doherty et al,[29] .

On the other hand, in this thesis only order of magnitude analysis of thermal stresses is considered to be important and a much simpler mean of calculating blade thermal stresses has been taken into consideration.

Assuming that there is no longitudinal temperature variation but there is only cross-sectional temperature variations in gas turbine blades and supposing constant modulus of elasticity,E,the thermal

stress on any one fiber of the unloaded blade at a particular section is ,

$$\sigma_i = E(\epsilon_i - \alpha_i T_i) \tag{71}$$

where, T_i and ϵ_i are local temperature rise and strain, respectively and α_i is the coefficient of linear expansion. Depending upon the geometry definitions given in Fig. 10, the force and moment balance equations about principal axes are expressed as,

$$\begin{aligned} \sum_{i=1}^{n} A_i \sigma_i &= 0 \\ \sum_{i=1}^{n} A_i \sigma_i x_i &= 0 \\ \sum_{i=1}^{n} A_i \sigma_i y_i &= 0 \end{aligned} \tag{72}$$

where A_i, σ_i and (x_i, y_i) are the area, stress and coordinates of ith fiber element, respectively and n is the number of elements.

Now, assuming that plane sections remain plane, we can write,

$$\epsilon_i = a + b x_i + c y_i \tag{73}$$

where a is the strain at the origin 0 and, [7]

$$\begin{aligned} a &= \frac{\sum_{i=1} A_i \alpha_i T_i}{\sum_{i=1}^{n} A_i} \\ b &= \frac{\sum_{i=1}^{n} A_i \alpha_i T_i x_i}{\sum_{i=1}^{n} A_i x_i^2} \end{aligned} \tag{74}$$

$$c = \frac{\sum_{i=1}^{n} A_i \alpha_i T_i y_i}{\sum_{i=1}^{n} A_i y_i^2} \tag{74}$$

Thus, combining equations (71), (73) and (74) yields,

$$\sigma_i = E\left(\frac{\sum_{i=1}^{n} A_i \alpha_i T_i}{\sum_{i=1}^{n} A_i} + x_i \frac{\sum_{i=1}^{n} A_i \alpha_i T_i x_i}{\sum_{i=1}^{n} A_i x_i^2} + y_i \frac{\sum_{i=1}^{n} A_i \alpha_i T_i y_i}{\sum_{i=1}^{n} A_i y_i^2} - \alpha_i T_i \right) \tag{75}$$

In above analysis centroid O of the blade section is the origin of the principal axes and so,

$$\sum_{i=1}^{n} A_i x_i = 0$$

$$\sum_{i=1}^{n} A_i y_i = 0 \tag{76}$$

$$\sum_{i=1}^{n} A_i x_i y_i = 0$$

On the other hand, for a simpler analysis the coefficient of thermal expansion can also be taken as temperature independent as modulus of elasticity E. Then equation (75) reduces to the form,

$$\sigma_i = E\alpha\left(\frac{\sum_{i=1}^{n} A_i T_i}{\sum_{i=1}^{n} A_i} + x_i \frac{\sum_{i=1}^{n} A_i T_i x_i}{\sum_{i=1}^{n} A_i x_i^2} + y_i \frac{\sum_{i=1}^{n} A_i T_i y_i}{\sum_{i=1}^{n} A_i y_i^2} - T_i \right) \tag{77}$$

In this thesis, equation (77) is used.

V. TURBINE BLADES

5.1 VARIOUS CHARECTERISTICS OF INVESTIGATED TURBINE BLADES

In order to clarify the subjects investigated in this thesis and to obtain the necessary data that will be utilized in analysing various aspects of cooled gas turbine blades, three different blades have been selected. Two of these are cooled blades with different cooling geometries and one is a solid blade resembling the extreme case. The existance of the solid blade in analysis is useful since it will provide the means to be compared with in the analysis of the cooling process in blades.

In the design of turbine blades the degree of the effectiveness of cooling geometry is determined by the shape factor Z whose expression can be given as, [30] .

$$Z = \left(\frac{S_c}{l}\right)^{1.2} \Big/ \left(\frac{A_c}{l^2}\right) \tag{78}$$

where l is the chord length of the blade and S_c and A_c are the perimeter and area of cooling passages, respectively. The Z values between 150 and 250 are required for good cooling.

In the selection of the turbine blades mentioned above, this fact

was taken into consideration and each blade was selected from a different class.Among the selected blades,BLADE-A (solid blade) is with zero Z factor,BLADE-B (pedestal blade) is with Z factor of 120 and the Z factor of BLADE-C (blade with elliptical cooling passages) is above 200.

The detailed geometries of the selected blades including the discretizations into elements are given in Fig.11,Fig.12 and Fig.13. The discretizations of the blades A,B and C are made of 33 quadratic elements with 122 nodes,29 quadratic elements with 127 nodes and 31 quadratic elements with 129 nodes,respectively.

The type of the blade material was assumed to be the same for all blades andit was taken as Inconel 600.Some properties of this material are given in Appendix C , Table 1.Although the thermal expansion coefficient and thermal conductivity are given as temperature dependent properties in Table 1,these parameters were assumed to be constants in the calculations.The reason for this assumption is to make the calculations simpler.Essentially,it does notgive rise to serious deviations from the exact solution.This fact has been investigated and presented by Hogge, [22] .The constant values of coefficients of thermal expansion and thermal conductivity are taken to be 1.44×10^{5} mm/(mm×°C) and 19.18 Joules/(sec×°C×m) ,respectively.

The external (gas to blade) heat transfer coefficient is geometry dependent and the variation of this coefficient with respect to blade geometry is given in Fig.14.This distribution has been derived from references [9] and [10] as to take the radiation effect into consideration.Fig.14 is valid for all blades considered in this thesis because the external geometries are the same in all three cases.The temperature of the gas flowing at the outer surfaces of the blades is 1145 °C.The characteristics of the convective exchange at the cooling passages for both cooled blades are given in Table 2.

VI. RESULTS AND DISCUSSION

The computer program FINEL solves the governing differential equation of the problem explained in Chapter I by using the finite element method and gives the temperature values at the nodes specified by the finite element meshes of the blades.The nodal temperatures have been calculated at 0,06 second time increments. The results of the computer program are utilized to examine the transient temperature behaviour at the stagnation point,mid point and trailing edge end of the blades,which are representative points as regards to stress.

In Fig,15,the transient temperature distributions of the stagnation point,mid point and trailing edge end of BLADE-A have been shown. It is seen that the stagnation point temperature increases at a decreasing rate.The temperature increase is roughly 400 °C/sec at 0,6 second and 110 °C/sec in the first two seconds of the start operation.This value decreases to 60 °C/sec after four seconds and 11 °C/sec after twenty seconds.

The trailing edge end temperature shows the same behaviour as the stagnation point does but the rate of change in temperature is very different at this point especially at early times.At the trailing edge end the average rate is about 650 °C/sec in the

first 0,6 second.This rate decreases to 125 °C/sec at two seconds and it is 80 °C/sec at four seconds.It reaches approximately to 2,5 °C/sec between twenty and twenty four seconds.At twenty four seconds the temperature of this point is 1135 °C.

On the other hand,at the mid point,the temperature is not changing for 0,6 second and it is remaining at the initial temperature of 20 °C.This is an expected result and the reason for it is that the inside part of the solid blade does not receive the effect of boundaries immediately.The diffusion of heat into the blade takes some time and only then the mid point temperature begins to rise. After 0,6 second,a linear variation of temperature is observed up to eight seconds.The rate of temperature increase is constant, 63 °C/sec,in the interval of two and eight seconds.The rate decreases to 12 °C/sec between twenty and twenty four seconds. At twenty four seconds the temperature of the mid point is 960°C. In the mean time,the maximum temperature differences between these three points are observed to appear at around four seconds. The temperature differences between the stagnation point and mid point and between mid point and trailing edge end are about 340°C and 630°C,respectively,at this time.These values reduce to 90°C and 180°C at twenty four seconds.

In Fig.16,the transient temperature distributions of the stagnation point,mid point and trailing edge end of BLADE-B have been illustrated.It is seen from this figure that the behaviour of temperature distribution of the stagnation point is similar to the one of BLADE-A.The temperature again increases at a decreasing rate,but in this case,the rate of increase is 125 °C/sec at two seconds, 75 °C/sec at four seconds and 5 °C/sec between twenty and twenty four seconds.When twenty four seconds of time is reached,the stagnation point temperature reaches to the value of 1010°C.

In contrast to the trailing edge end the temperature distribution of BLADE-A,the temperature distribution of the corresponding point of BLADE-B is not so gradual.At the times of 0,6 ,one two,four and eight seconds,the rates of increase in temperature are 1160 °C/sec,830 °C/sec,40 °C/sec,7 °C/sec and 0 °C/sec respectively.According to these values at the trailing edge end

of BLADE-B,the temperature is at the steady state condition after eight seconds,The steady state temperature of this point is 975°C. Surprisingly,this temperature is below the temperature of the stagnation point temperature after twenty four seconds,This fact is surprising because if the geometries of the leading edge and trailing edge are considered,with its small thickness and large heat transfer surface,the trailing edge should be at a higher temperature even in steady state conditions,Whereas,the film cooling passage placed at the trailing edge whose cooling effectiveness is higher than the cooling passage at the leading edge compensates the effect of large heat flux,It even keeps the temperature at this location under the leading edge temperature in steady state conditions.

The mid point temperature distribution in BLADE-B has the lowest temperature values at all times as it is in BLADE-A,However, in this case the initial behaviour of this point is not similar to the one in case of BLADE-A,The time at which the effect of heat flux diffusing into the blade is received,is so small that it is not possible to observe it on the curve,This also means that this value is even less than time increment value(0,06 second).The temperature at this point gradually increases to a maximum of 810°C at twenty four seconds.The temperature changes more or less linearly up to three seconds and the rate in this interval is 110 °C/sec.At four seconds,this value decreases to 75 °C/sec and between twenty and twenty four seconds it is 2,5 °C/sec.The temperature differences between these three points are much severer in this case.At two seconds the temperature difference between mid point and trailing edge end is about 700°C and this is the maximum difference that occurs.At this particular time the temperature difference between the stagnation point and the mid point is 200°C.On the other hand,while the difference between the stagnation point and mid point remains constant in time,after two seconds the difference between the mid point and the trailing edge end decreases continiously in time and reaches to a value of 150°C at twenty four seconds.

The transient temperatures at the three locations, the stagnation point,the mid point,and the trailing edge end,in BLADE-C are given in Fig.17,It follows from the figure that the stagnation point temperature keeps its gradually increasing behaviour with a decreasing rate in case of BLADE-C,too.But in this case,there is one point differing from the previous cases that the stagnation temperature seems to reach the steady state at sixteen seconds.In BLADE-C the rates of increase of the stagnation point temperature are 380 °C/sec,200 °C/sec,125 °C/sec and 70 °C/sec at the times 0,6,one,two,and four seconds,respectively.The rate is zero between twenty and twenty four seconds which means that in this interval the temperature reaches to the steady state value of 930°C.

In BLADE-C,the trailing edge end temperature behaves as in case of BLADE-B.A rapid increase in temperature is observed first and then suddenly the temperature reaches to the steady state value. Up to 0,6 second a linear increase in the temperature exists at this point with the rate of increase of 950 °C/sec,Thenon,at time one second the rate is 700 °C/sec,at time two seconds the rate is 125 °C/sec and at time four seconds the rate is 30 °C/sec.After ten seconds the rate of temperature increase is zero and the temperature remains at this steady state value of 1055°C.

When the mid point temperature variation in time is observed in Fig.17,at the beginning, the existance of a portion with an increasing rate is determined.This fact is due to the time elapsed until the heat transferred into the blade is received by this point.But unfortunately it is not possible to determine this time interval in this case as clear as in case of BLADE-A.After this point,the transient temperature curve of the mid point is smoothly increasing but again decreasingly as in two previous cases.The temperature increase rates are 70 °C/sec,90 °C/sec,75 °C/sec and 2.5 °C/sec between zero and one,one and two,at four seconds and between twenty and twenty four seconds,respectively.The mid point temperature at twenty four seconds is 750 °C.The maximum temperature difference between the mid point and the trailing edge end seems to occur at two seconds in Fig.17,This value is about 710°C. On the other hand,at this particular time the temperature differ-

ence between the mid point and the stagnation point is 290°C, According to Fig,17 as time passes,the temperature difference between the mid point and the trailing edge end reduces continiously while the difference between the mid point and the stagnation point increases to 300°C first and then decreases continiously.At twenty four seconds the differences are 310°C between the mid point and trailing edge end and 170°C between the mid point and the stagnation point.

If the temperature is taken as the only design parameter and if the result analysis given above is considered,it is easy to observe that BLADE-A can not be used under the specified conditions of the thesis,This is based on the fact that in this blade the temperature is changing at all points continiously in time up to the external gas temperature and as it was mentioned before the external gas temperature has taken to be the ultimate temperature that the blade material,Inconel 600,can withstand.On the other hand,in the cooled blades B and C the temperature is much lower than the external gas temperature at most part of the blades when they reach the steady state,Only at the trailing edge of BLADE-C the temperature is critical and it is just 100°C less than the external gas temperature,At the trailing edge end of BLADE-B this value is about 175°C and at any other point at the trailing edge of BLADE-B,this temperature difference is higher in comparison to the corresponding points of BLADE-C,The overall cooling effectiveness of BLADE-C is the highest but at the trailing edge the cooling is less in comparison to the trailing edge of BLADE-B,Thus,it can be concluded that although the ovrall cooling effectiveness is higher in BLADE-C,the local cooling effectiveness of its trailing edge geometry is less than a film cooling geometry as it is contained in BLADE-B,At the leading edge and mid portion,the cooling process is much more effective in BLADE-C than in BLADE-B as it is concluded from the results,At the leading edge,the temperature is about 250°C in BLADE-C while it is about 150°C in BLADE-B.

In figures 18,19 and 20 the isoterms in blade sections are presented at the times 1,5,12 and 22 seconds,respectively.In Fig.18 the temperature distributions in sections of blades A,B and C at the time 1,5 seconds are shown.According to this figure,at the

leading edge and mid portion of BLADE-A the temperature is a little higher than 300°C.These portions are surrounded by the 300°C isoterm just inside the blade boundary except a portion of the pressure side.On the pressure side the temperatures are lower than the suction side temperatures and on this portion of the boundary it is a little higher than 200°C.As one goes inwards the temperature reduces gradually and the lowest isoterm is reached near the mid portion. This isoterm has a value of 60°C.Besides,at the trailing edge,the temperature is rather high and 300°C isoterm is followed by 350°C 400°C and 500°C isoterms as it is come near to the trailing edge.

On the other hand,in blades B and C the variations of the isoterms are not as clear as the ones in BLADE-A.Only it can be talked about the general trends.The reason for such a behaviour is the cooling of these blades.By the cooling process on various portions of these blades,different cooling conditions are imposed.Together with the external heat transfer coefficient distribution,these conditions distroy the simplicity of the temperature distributions inside the blades.

In both blades the suction sides are hotter than the pressure sides as it was in BLADE-A.In BLADE-B,just inside the boundary 400°C isoterm takes place and it extends from quite above the stagnation point to the trailing edge.On most of the pressure side the isoterms are below 300°C.This limit is exceeded on the leading edge and on the portions of the mid part near the trailing edge.As one comes near the trailing edge end higher isoterms appear which extend transverslly and reach to the maximum of 800°C.The coolest parts are the regions between the first and the third cooling passages.In this region the temperature is around 200°C.

In BLADE-C the large portion of the suction sidé is at 400°C and 400°C isoterm extends from above the stagnation point to the trailing edge.But in this blade there is one exceptional region on which the temperature even exceeds 500°C on the suction side of the leading edge.The trailing edge temperature distribution is similar to the corresponding part of BLADE-B but in this case the hot region is rather large.In this region the isoterms begin with 500°C and

end with 800°C,One other important point that should be mentioned here is the existance of a large cool region in the mid portion of BLADE-C,In this region the temperature is below 200°C and there is even a region in which temperature is below 120°C,

The temperature distributions in the sections of blades A,B and C at the time twelve seconds are presented in Fig,19,In this figure it can be seen that in BLADE-A the hot trailing edge region is diffusing towards the mid portion,Therefore the cooler isoterms extending from the leading edge to the trailing edge at time 1,5 seconds now surrounds only the mid portion,The hottest region is the trailing edge,At this location the isoterms are between 900°C and 1080°C,The coolest region is in the mid part of the blade and it is surrounded by 650°C isoterm,In BLADE-B the isoterms are clearer at this instant of time,Now they are long longitudinal lines,900°C isoterm surrounds a large portion of the blade,including most of the leading edge and all of the mid portion,Only the trailing edge is excluded by this isoterm,At the leading edge there is a region hotter than 920°C,On the other hand,the coolest regions are again the ones between the first and the third cooling passages. 750°C isoterm seems to bound the coolest region in BLADE-B,At the trailing edge,950°C isoterm is the most significant one,The temperature is 968°C near the trailing edge end,In BLADE-C the complicated behaviour of isoterms remains at this instant,Approximately the distribution of isoterms is the same as in Fig,18,The hot region on the suction side above the stagnation point is still there and it is now bounded by 900°C isoterm,The mid portion is still the coolest region and the temperature of this region is the lowest among all three blades,This region has a temperature of 650°C as the lowest,The trailing edge distribution is also the same except the change in the magnitudes of isoterms,In this region the isoterms take the values between 900°C and 1040°C as one proceeds towards the trailing edge end,

In all three sections the pressure sides are cooler than the suction sides,This fact is the consequance of the heat transfer distribution on the blade surfaces,The distribution considered in this thesis is given in Fig,14,In this figure it is observed that the

suction side heat transfer rate is generally higher on every location corresponding to that of the pressure side.This stems from some aerodynamic phenomenon existing in the cascades,as demonstrated recently by Graziani et al. 27 ,Consigny et al. 28 and by many others in past.

Fig.20 contains blades A,B and C with their temperature distributions at the time twenty two seconds. After this time the temperature distributions are expected to reach the steady state.The distribution of isoterms in BLADE-A at this instant is exactly the same as the distribution in the time of twelve seconds given in Fig.19.Only the magnitudes are different and they are higher in this case.At the leading edge 1020°C isoterm is the highest.The coolest region of this blade is again in mid portion and it is bounded by 950°C isoterm.The enlargement of the hot trailing edge region seems to stop which means that the steady state values are close.In the trailing edge the isoterms are between 1060°C and 1130°C.1130°C is very close to the external gas temperature which is 1145°C.

In BLADE-B and BLADE-C enlargements in cool portions of the mid part are observed.This also means that both blades have almost reached the steady state.In BLADE-B the coolest region is surrounded by 850°C isoterm while in BLADE-C the temperature in the same region is about 750°C at a large portion.The highest leading edge isoterms are 990°C and 900°C in BLADE-B and BLADE-C,respectively. The hot region appearing on the suction side of BLADE-C above the stagnation point at times 1.5 seconds and twelve seconds does not exist anymore.At the trailing edge of BLADE-B the isoterms are all longitudinal now and the highest is 980°C isoterm.But at the same location of BLADE-C the complicated behaviour of isoterms remains and the highest temperature is above 1040°C in this case.

The results of the thermal stress analysis that has been carried out in this thesis are presented in the same order as the thermal field analysis.Therefore the first illustrations belong to the transient thermal stress distributions.Figures 21,22 and 23 illustrate the transient thermal stresses in blades A,B and C.

Fig.21 contains the calculated stress distributions in BLADE-A during the starting operation for the stagnation point,mid point and the trailing edge end.It may be followed from the figure that there are two curves behaving similarly and only differing in magnitude.These curves are the ones that belong to the stagnation point and the trailing edge end.Both curves have their maxima at the time equal to two seconds.The magnitudes are -195 MPa for the stagnation point and -310 MPa for the trailing edge end.The third curve is illustrating the thermal stress variation of the mid point.This curve also has its maximum at about two seconds.This is a very expected manner because as it was mentioned in the previous thermal field results,two seconds is the time at which the temperature gradients reach their maximum values.Just as the temperature distribution,the rate of change of stress is high at the beginning and it decreases in time.The maximum differehce in stresses of the three points is at two seconds.The difference is 450 MPa between the mid point and the trailing edge end.This difference decreases to 60 MPa at twenty four seconds and the tendency to decrease continues.In spite of the high rate of change in stress at the beginning the distribution of stresses is quite smooth.

Fig.22 is the figure presenting transient stress distributions in BLADE-B at the stagnation point,mid point and trailing edge end. The stress variation at the mid point of this blade is exactly the same as in BLADE-A,even in magnitude.Therefore there is no need to discuss this curve.But on the other hand,the behaviours of the other two points,the stagnation point and the trailing edge end,are quite different.At the trailing edge there is a very sudden increase in stress in a compressive manner in the first second and in this period the stress reaches a value of -390 MPa.Then a rapid decrease in stress at this point is observed and it reaches a value of -100 MPa at four seconds and a value of 0 MPa at eight seconds.From that time onwards the stress at this point is tensile and has a maximum of 40 MPa.In contrast,the rate of change of stagnation point stress is rather small and at this point the stress reaches to its maximum,namely -75 MPa,at about two seconds.From there on,it is observed that the stress increases at this point and it reaches a value of 0 MPa at fifteen seconds.At later times the stress has a

constant value of 8 MPa,The maximum stress difference appears again between the mid point and the trailing edge end at about two seconds and its magnitude is 500 MPa.

The transient stress distributions of the stagnation point,mid point and the trailing edge end of BLADE-C are given in Fig.23,The behaviour of stress at the mid point is again the same as it is in two previous blades.In this case only its magnitude is higher.During the start operation,at the trailing edge,a sudden increase in stress appears also in this blade,The stress is in compressive manner but it is higher compared to the stresses at the corresponding points of the other two blades,It has a value of -400 MPa.Besides,the rate of change of stress is not as high as in other two cases after the peak value,The stress decreases slowly up to -200 MPa which is at a time of seventeen seconds and then it increases again.At the stagnation point,an increase in stress with rather low rates of change up to fifteen seconds,From thereon,an increase in stress is observed at this point,too.

In fig.24,Fig.25 and Fig.26 the stress distributions in blades A,B and C are presented at the times 1.5,twelve and twenty two seconds respectively,According to these figures in all three blades and at all times there are central portions surrounded by neutral stress contours. Inside these contours one observes tensile stresses.Whereas as one proceeds towards the skin of the blades the stresses become compressive.This observation is valid at all times,However,this fact is expected because the skin temperatures of all three blades are always higher than the inner temperatures,Thus the outer fibers of the blades have more tendency to extend than inner fibers.So,while outer fibers exert tensile stresses on inner fibers,inner fibers exert compressive stresses on outer fibers of the blades.

On the other hand,there is another fact that generally on the pressure sides of the blades tensile stresses exist.But on the suction sides it is always observed that the stresses are compressive.This is also an expected behaviour.As it is observed in temperature analysis of blades,the suction side temperatures are always higher

than the pressure side temperatures,But this means that the suction side fibers of the blades tend to extend more than the pressure side fibers,Hence,while the suction side fibers exert tensile stresses on the pressure side fibers,they exert compressive stresses on the suction side fibers of the blades.

Besides these general trends in the blades,individual variations are also observed,For instance,at the trailing edge of BLADE-B,at a time of 1,5 seconds high compressive stresses are observed.But these stresses disappear at a time of twelve seconds and they reach values having the order of magnitude of 30 MPa,From thereon they remain constant,Whereas in BLADE-C,high compressive stresses always exist at the trailing edge with the order of magnitude of -300 MPa.The leading edge and the mid portion of the blades have more or less the same stresses at all times,The reason for the existance of high stresses,either tensile or compressive,is the high temperature gradients existing on different portions of the blades,For instance in BLADE-C,the gradient is 380 °C/sec at the stagnation point , 950 °C/sec at the trailing edge end and 70 °C/sec at the mid point at 0,6 second,This obviously gives rise to large temperature differences between these portions in a very small period of time.In fact at two seconds the temperature difference between the mid point and the trailing edge end is 710°C,This very high difference is the cause of a very high thermal stress.

As it is followed from the temperature analysis,the coolest and the hottest regions are observed in BLADE-C,Therefore the highest thermal stresses appear in this blade.In order to eliminate these stresses either the cool regions may be warmed up or the hot regions may be cooled down,The existance of the cool regions are desirable and they are the goals of cooling process by which the material of the blade is saved,Thus,the hot regions should be cooled down.This solution can be achieved by choosing a more effective cooling geometry particularly for these regions,When the cooled blades of this thesis are investigated it is seen that the leading edge and the mid portion of BLADE-C are cooler than the corresponding portions of BLADE-B,But in contrary,the trailing edge of BLADE-B has more effective cooling geometry than the similar portion of BLADE-C.

Consequently,the combination of the various cooling geometries of the two blades which are the most effective geometries may create the most convenient blade.Depending upon the preceeding analysis and above conclusion,it can be proposed that BLADE-C with a film cooled trailing edge will be the most convenient.An example of such a blade is given in Fig.27.In this blade since the temperature gradient between the mid point and the trailing edge end will decrease the thermal stresses will be reduced.In the mean time,presumably the maximum temperature of the trailing edge in BLADE-C will also be reduced.In such a case,the lowest difference between the blade temperature and the external gas temperature will be of the order of magnitude of 250°C.This means that even if the gas with temperature higher than the allowable material temperature is used the blades of the turbine will not be destroyed due to high temperature effect.

VII. CONCLUSIONS

In this thesis features of the transient temperature distribution in turbine blades were examined in detail,using finite element method.The following was concluded:

1. Finite element method solves heat transfer problems accurately even if the geometry is very complex,Hence,it is one of the best methods to solve heat transfer in blades when very complex geometries of cooled blades are considered.

2. In a transient heat conduction problem,application of finite element method to space coordinates and finite difference method to time coordinate establishes an easy and accurate combination.

3. Cooled blade is a powerful tool in cases where one has to increase the external gas temperature as high as possible and to keep blade temperature as low as possible,But in the design of cooled blades,thermal stresses must always be taken into consideration.For some cooled blades thermal stress problem is very serious eventhough they have high cooling effectivenesses.This is the case for BLADE-C investigated in this thesis.

4. Besides overall cooling effectiveness,local cooling effectiveness is also an important parameter.Even if most of the blade is effectively cooled,existance of less cooled parts causes problems by giving rise to high temperature differences in the blade and so,

creating high thermal stresses,This fact was realized in the analysis of BLADE-C,

5. During start and shut-down operations of gas turbines transient temperature distributions become very complicated,In these periods temperature gradients are very high both in chordwise direction and between the skin and core region of a blade,Because of these high gradients magnitudes of thermal stresses in blades are also very high in these periods,

BIBLIOGRAPHY

1. MUKHERJEE,D.K., "The Cooling of Gas Turbine Blades", Brown Boveri Rev.,Vol. 64,n1,pp.47-51,1977.

2. EMERY,A.F. and CARSON,W.W., "An Evaluation of the Use of the Finite Element Method in the Comput tion of Temperature" , ASME Paper No.69-WA/HT-38.

3. GURTIN,M.E., "Variational Principles for Linear Initial Value Problems" ,Quart. Appl. Math.,Vol.22,p.252,1964.

4. HUEBNER,K., "The Finite Element Method for Engineers" ,John Wiley and Sons,New York,1975.

5. KOHLER,H.,HENNECKE,D.K.,PAFF,K. and EGGEBRECHT,R., "Hot cascade Test Results of Cooled Turbine Blades and Their Application to Actual Engine Conditions" ,50th AGARD-PEP Symp. on High Temp. Prob. in Gas Turbine Engines,Ankara,Turkey,Sept.19-23,1977.

6. CAMCI,C., "Temperature Analysis of Cooled Gas Turbine Blades Under Steady-State Conditions" ,M.Sc. Thesis,Bogaziçi University Istanbul,1980.

7. MUKHERJEE,D.K., "Stresses in Turbine Blades Due to Temperature and Load Variation" ,ASME Paper No. 78-GT-158,1978.

8. BARNES,J.F. and FRAY,D.E., "Some Aspects of Research at the National Gas Turbine Establishment on Internally Air Cooled Turbine Blades" ,Proc. Inst. Mech. Engrs.,178,Part 3I,p.53,1964.

9. COLLADAY,R.S., "Turbine Cooling" ,Turbine Design and Application, ed. Glassman,A.J.,NASA SP-290,Vol.3,pp.68-99,Washington,1975.

10. MUKHERJEE,D.K. and FREI,O., "Temperature Measurements on Cooled Gas Turbine Stator Blades" ,ASME Paper No. 74-GT-31,1974.

11. CONSIGNY,H. and RICHARDS,B.E., "Short Duration Measurements of Heat Transfer Rate to a Gas Turbine Rotor Blade" , ASME Paper No. 460-GT-80,1980.

12. GRAZIANI,R.A.,BLAIR,M.F.,TAYLOR,J.R. and MAYLE,R.E, "An Experimental Study of Endwall and Airfoil Surface Heat Transfer in a Large Scale Turbine Blade Cascade" ,Journal of Engineering for Power,Vol.102,1980.

13. POLLMANN,E., "Temperatures and Stresses on Hollow Blades for Gas Turbines" ,NACA TM 1183,1947.

14. PANTELEEV,A.A. and TRUSHIN,V.A., "Calculation of Transient Temperature Fields in Cooled Blades in Turbines" ,Teploenergetica 21(8)33-35,1974.

15. ZIENKIEWICZ,O.C., "The Finite Element Method in Engineering Science" ,McGraw-Hill Publ. Company,Inc.,New York,1971.

16. ZIENKIEWICZ,O.C. and CHEUNG,Y.K., "Finite Elements in Solution of Field Problems" ,The Engineer,220,495-510,1965.

17. WILSON,E.L. and NICKEL,R.E., "Application of Finite Element Method to Heat Conduction Analysis" ,Nuclear Engg. and Design, Vol.51,pp.389-401,1979.

18. ZIENKIEWICZ,O.C. and PAREKH,C.J., "Transient Field Problems: Two-dimensional and Three-dimensional Analysis by Isoparametric Finite Elements" ,Int. J. for Num. Meth. in Engg.,Vol.2 pp.61-71,1970.

19. GALLEGER,R.H. and MALLET,R.H., "Efficient Solution Process for Finite Element Analysis of Transient Heat Conduction" ,ASME Paper No. 69-WA/HT-39.

20. BRUCH,J.C. and ZYVALOSKI,G., "Transient Two-dimensional Heat Conduction Problems Solved by the Finite Element Method" , Int. J. for Num. Meth. in Engg.,Vol.8,pp.481-491,1974.

21. KOHLER,W. andPITTR,J., "Calculation of Transient Temperature Fields with Finite Elements in Space and Time Dimensions" , Int. J. for Num. Meth. in Engg.,Vol.8,pp.625-631,1974.

22. HOGGE,M.A., "Thermal Fields and Stresses in Cooled Turbine Blades by the Finite Element Method" ,Lecture Series on Cooled Turbine Blades,von Karman Inst.,Jan. 12-16,1976.

23. ERGATAUDIS,I.,IRONS,B.M. and ZIENKIEWICZ,O.C., "Curved,Isoparametric,Quadrilateral Elements for Finite Element Analysis", Int. J. of Solids Structures,Vol.4,pp.31-42,1968.

24. DAVIS,P.J. and RABINOWITZ,P., "Methods for Numerical Integration" Academic Press,Inc.,New York,pp.268-273,1975.

25. SIEGERLIND,L.J., "Applied Finite Element Analysis" ,John Wiley and Sons,Inc.,1976.

26. BATHE,K.J. and KHOSHGOFTAAR,M.R., "Finite Element Formulation and Solution of Non-linear Heat Transfer" ,Nuclear Engg. and Design,Vol.51,pp.389-401,1979.

27. BOLEY,B.A. and WEINER,J.H., "Theory of Thermal Stresses" , John Wiley and Sons,Inc.,New York,1960.

28. GATEWOOD,B.E., "Thermal Stresses" ,McGraw-Hill Book Company, New York,1957.

29. DOHERTY,W.P.,WILSON,E.L. and TAYLOR,R.L., "Stress Analysis of Axissymmetric Solids Utilizing Higher Order Quadrilateral Finite Elements" ,Structural Engg. Lab.,University of California, Berkeley,1969.

30. HORLOCK,J.H., "Axial Flow Turbines" ,Kruger Publ. Co.,1973.

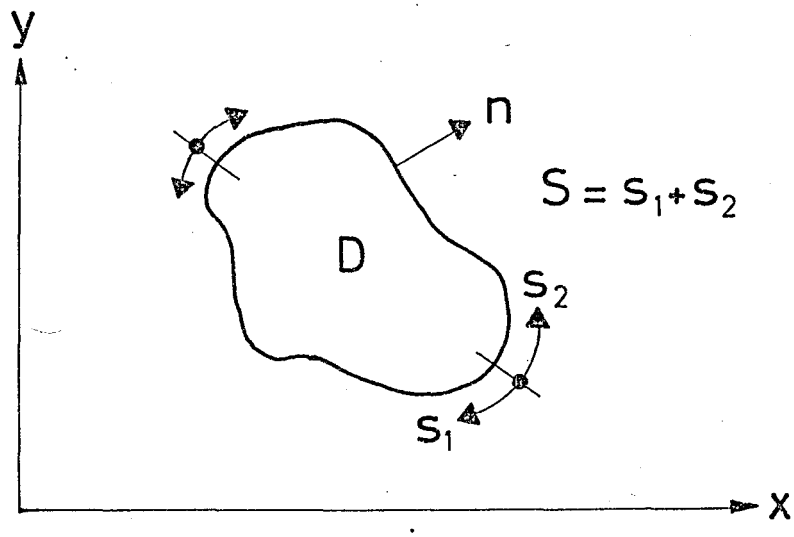

FIG.1- Solution Domain for General Two-dimensional Heat Conduction.

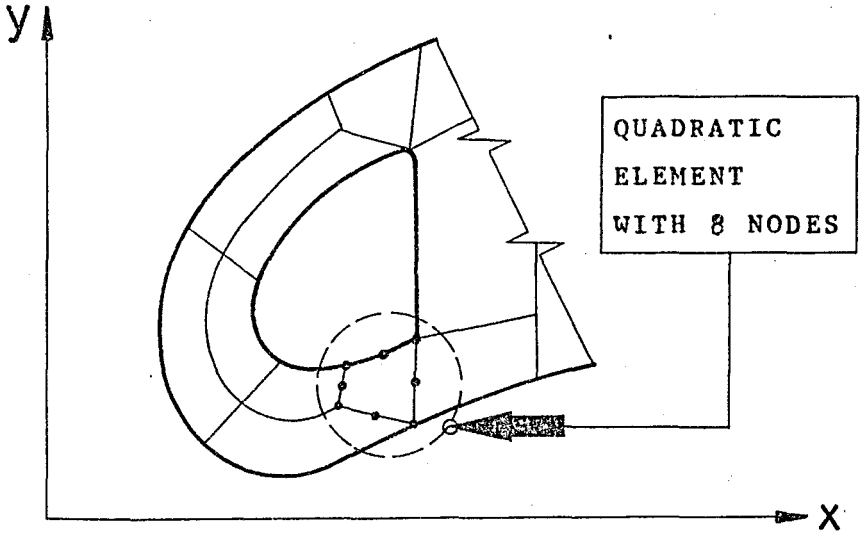

FIG.2- A typical quadratic element used in the thesis.

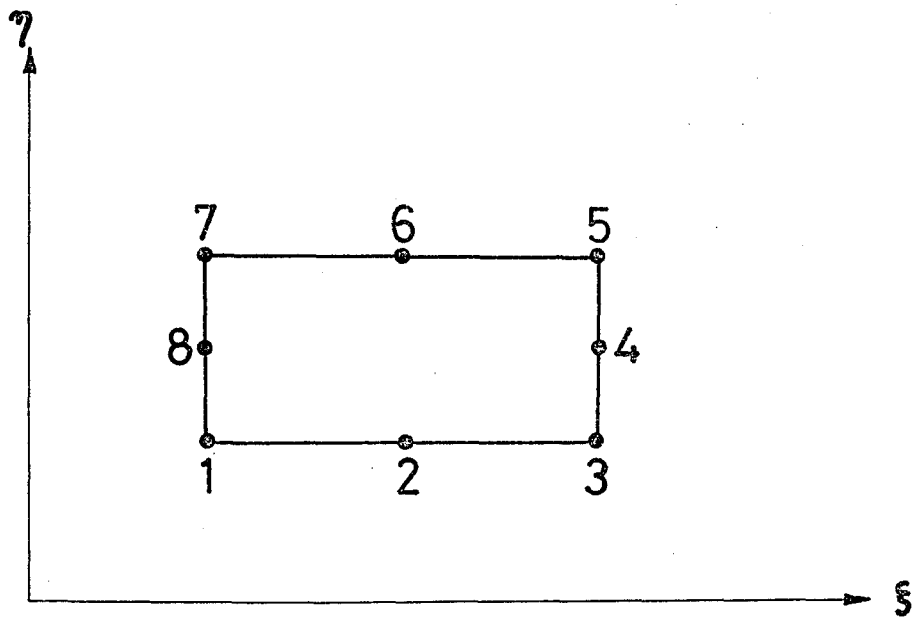

FIG. 3- A rectangular quadratic element in the transformed domain.

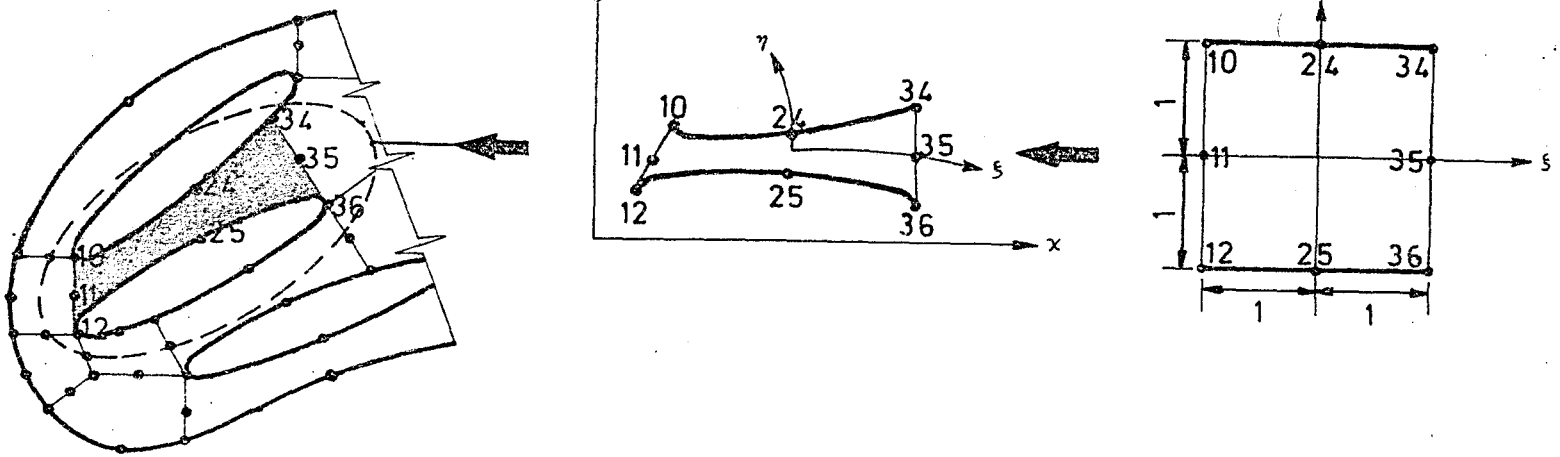

1) A blade section with elements and nodes

2) The global coordinate system for an element in the section.

3) The local coordinate system for the same element

FIG.4- The transformation of a typical element from local coordinates to global.

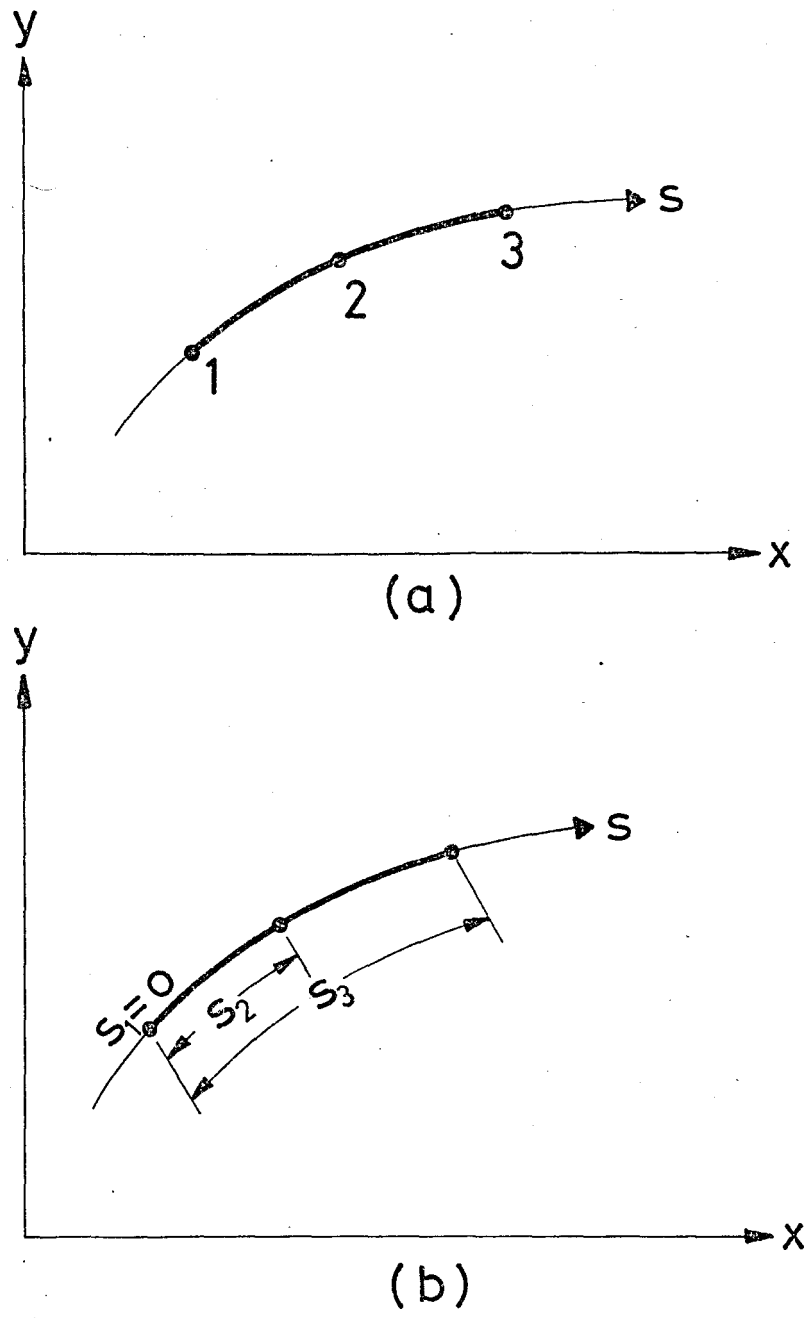

FIG.5 - One-dimensional quadratic finite element and the terminology used in line integrals.

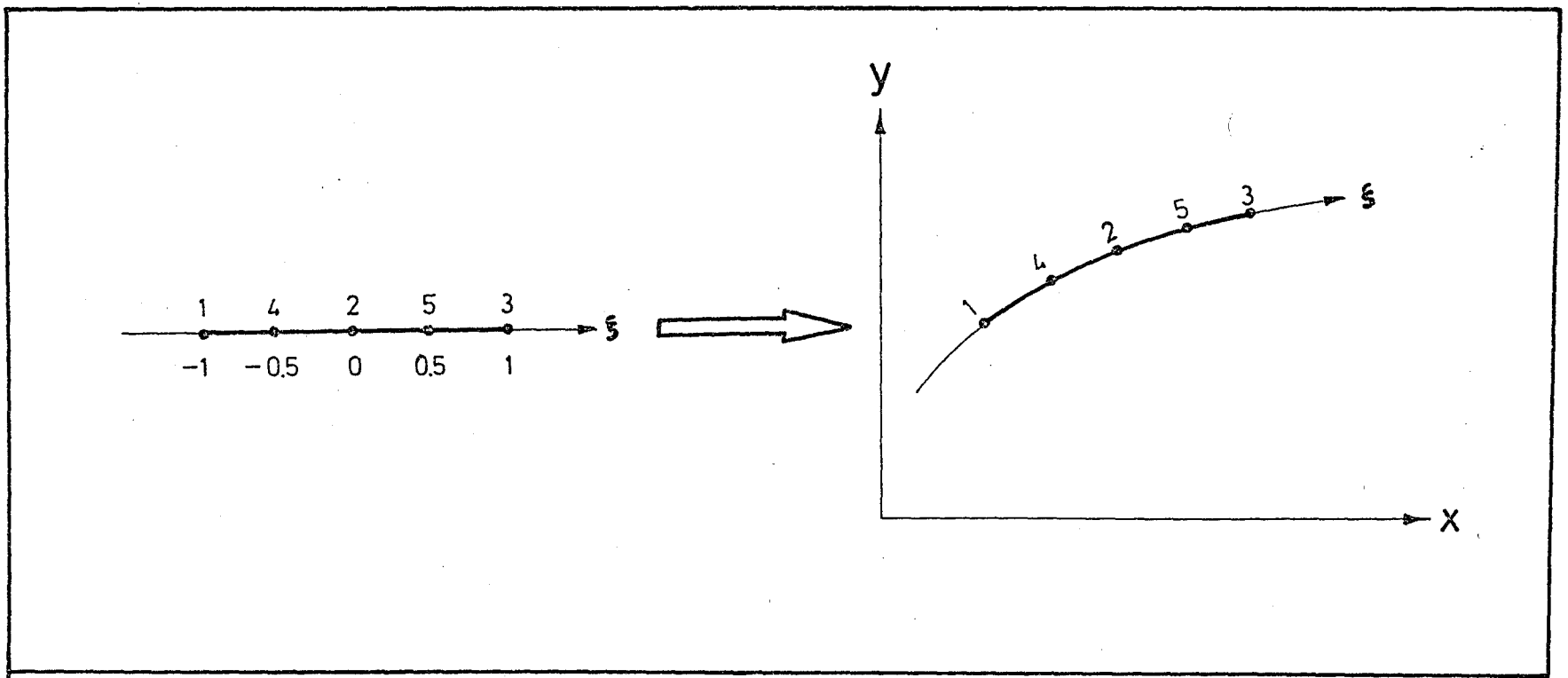

FIG.6- Isoparametric transformation of one-dimensional quadratic finite element.

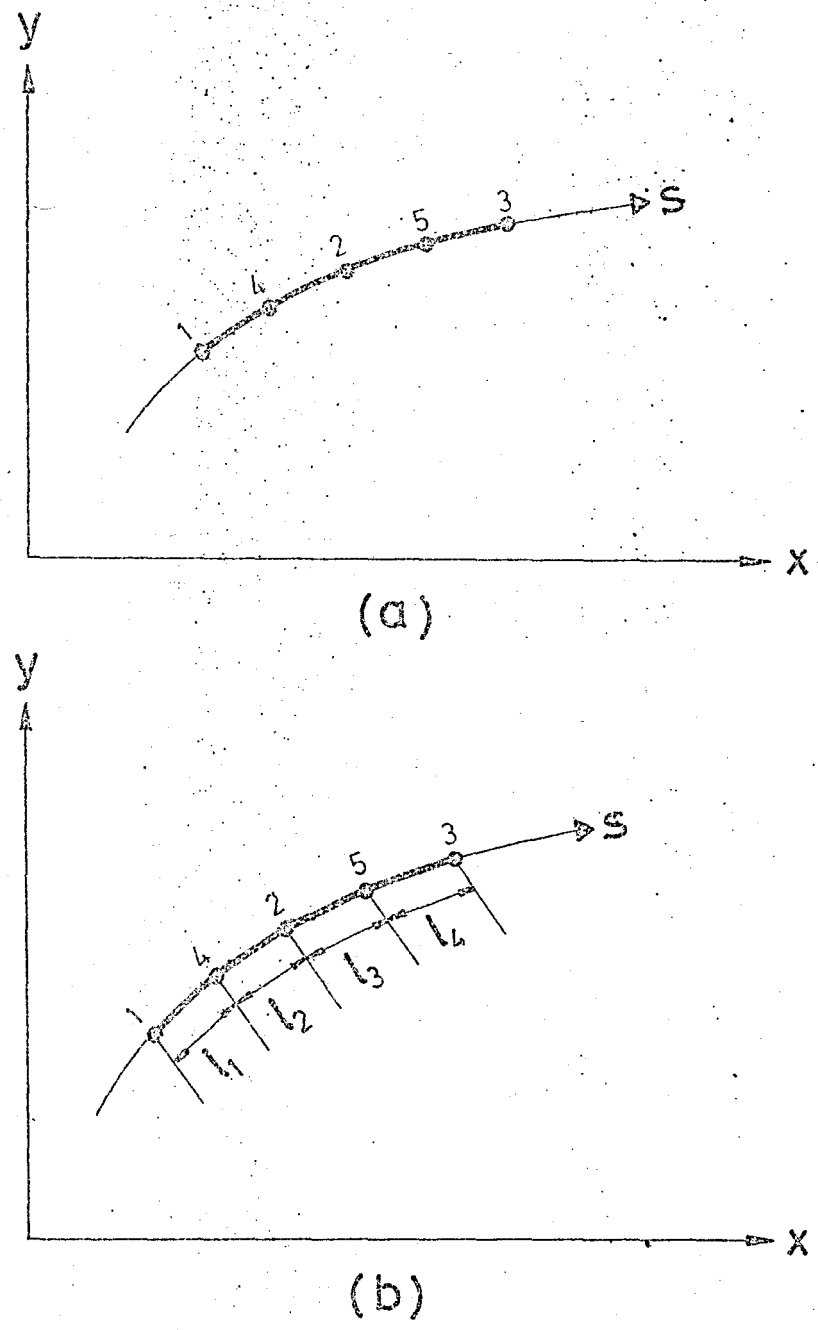

FIG.7- Approximation of a curve by line segments.

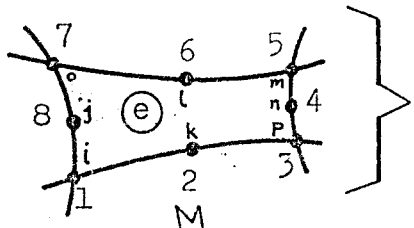

1,2,3,4,5,6,7,8 are local node numbers, i,j,k,l,m,n,o,p are global node numbers of element "e".

$$\begin{bmatrix} a_{11} & & a_{13} & & & a_{16} & & a_{18} \\ & & & & & & & \\ a_{31} & & a_{33} & & & a_{36} & & \\ & & & & & & & \\ & & & & & & & \\ a_{61} & & a_{63} & & & a_{66} & & \\ & & & & & & & \\ a_{81} & & & & & & & a_{88} \end{bmatrix} \quad [A]^{(e)} \qquad [F]^{(e)} \begin{bmatrix} f_1 \\ \vdots \\ f_3 \\ \vdots \\ f_6 \\ \vdots \\ f_8 \end{bmatrix}$$

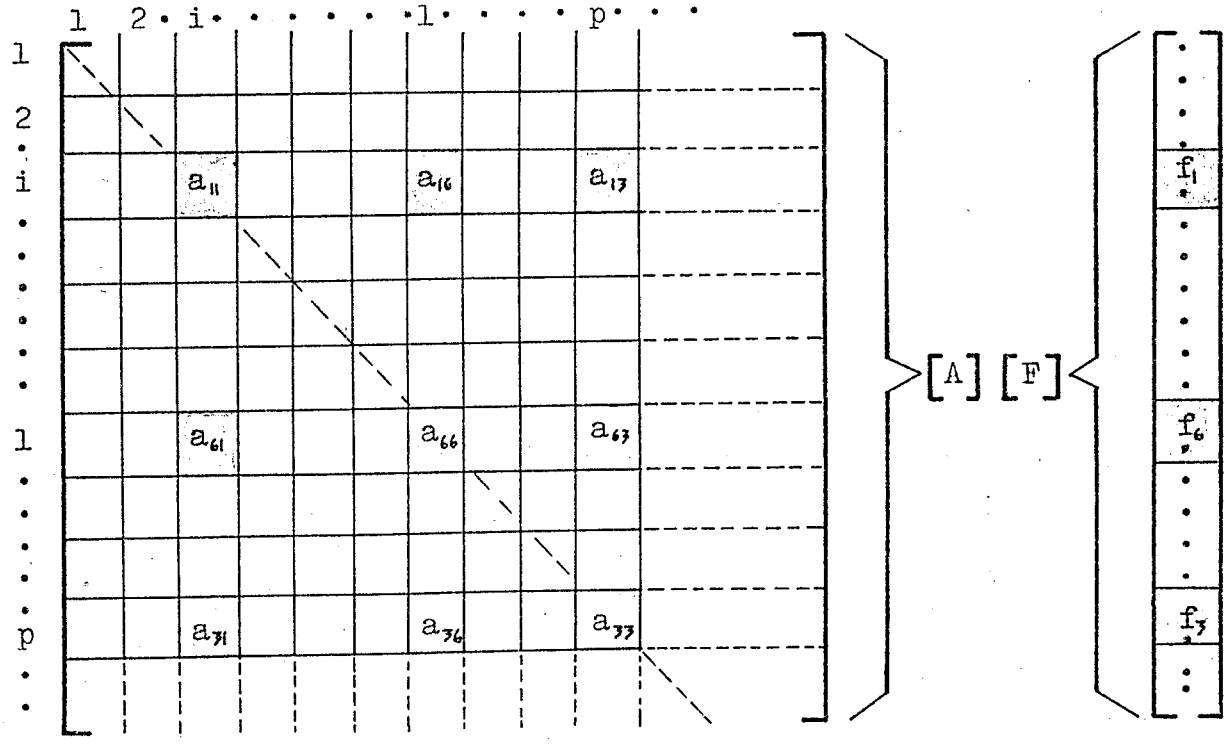

FIG.8- Assemblage of global matrices.

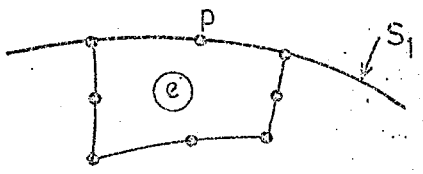

BOUNDARY CORRECTION

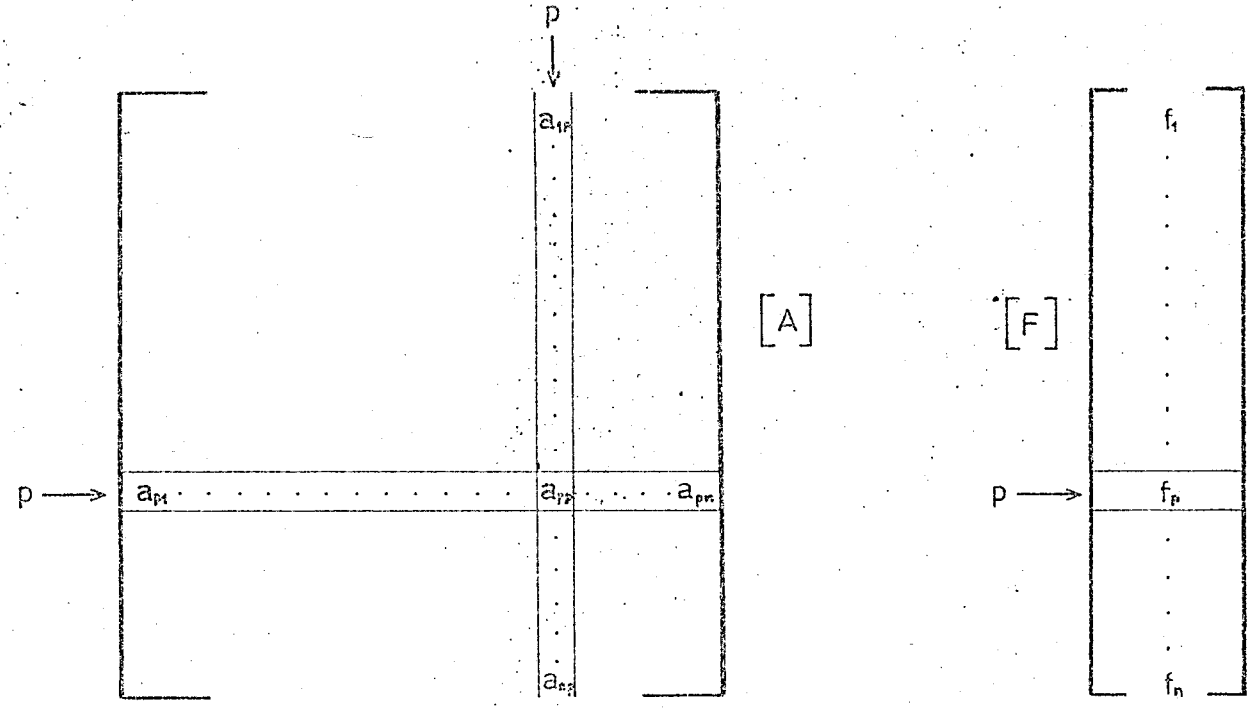

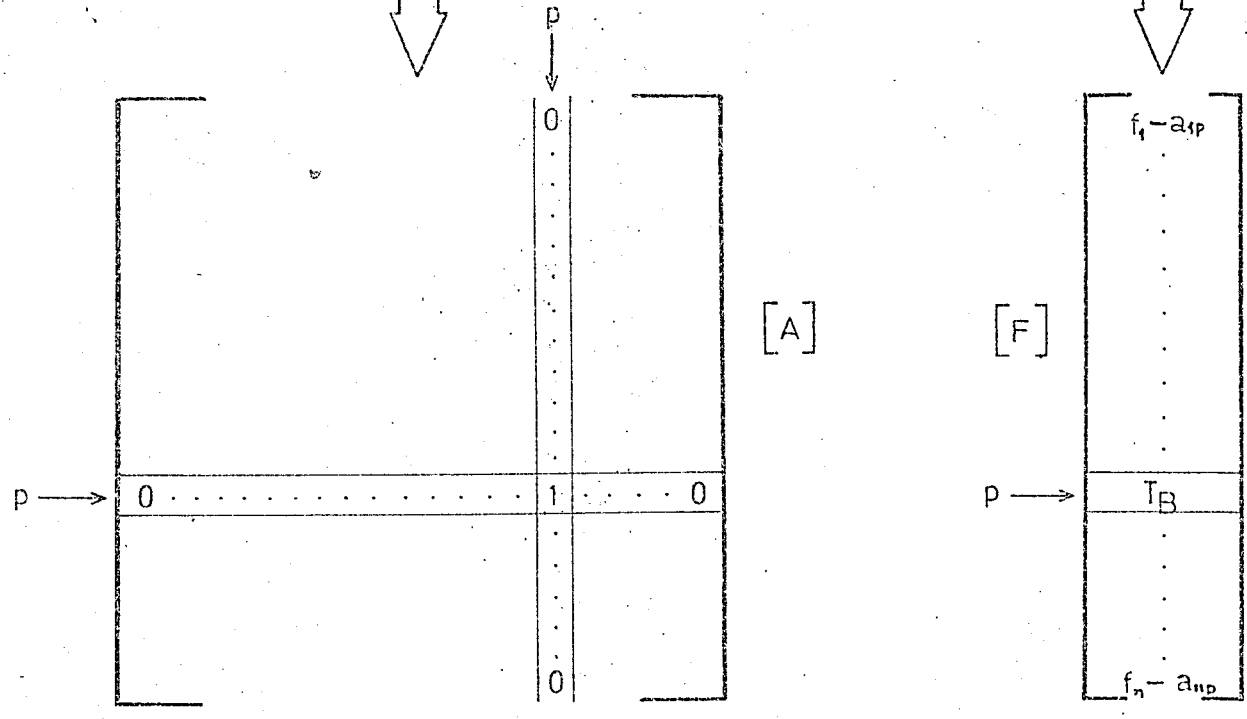

(Continued).

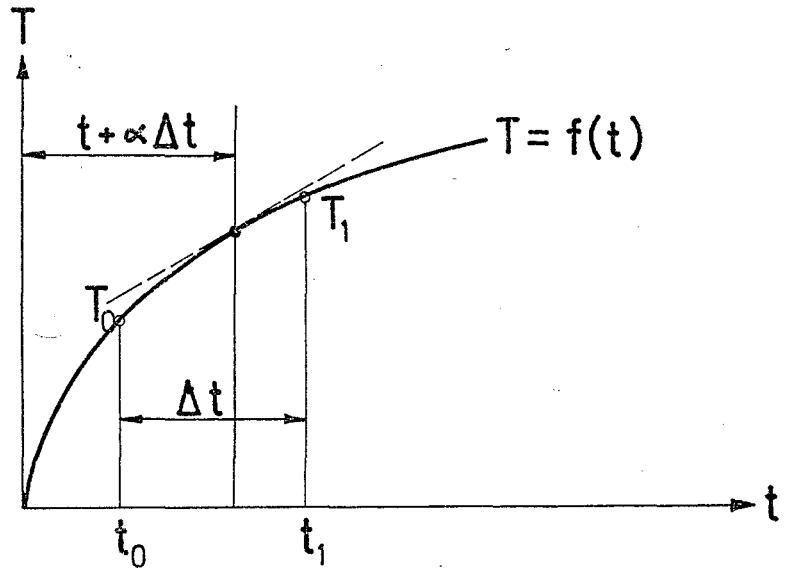

FIG.9- Integration of field variable T in time domain.

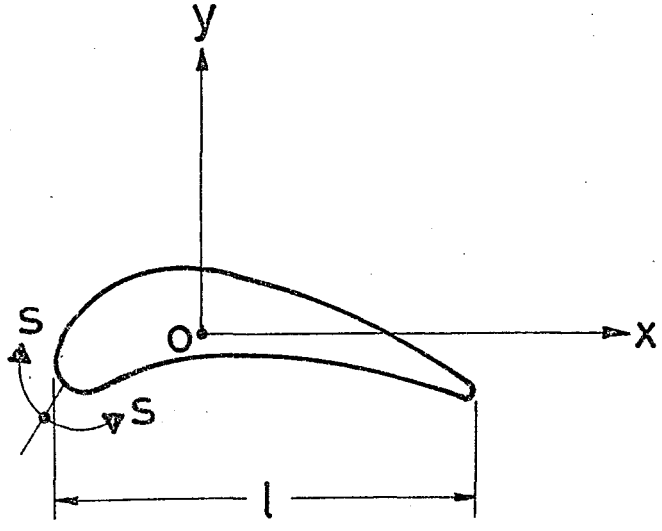

FIG.10- The blade section defining geometry used in thermal stress calculations where O is the centroid and x and y are principal axes.

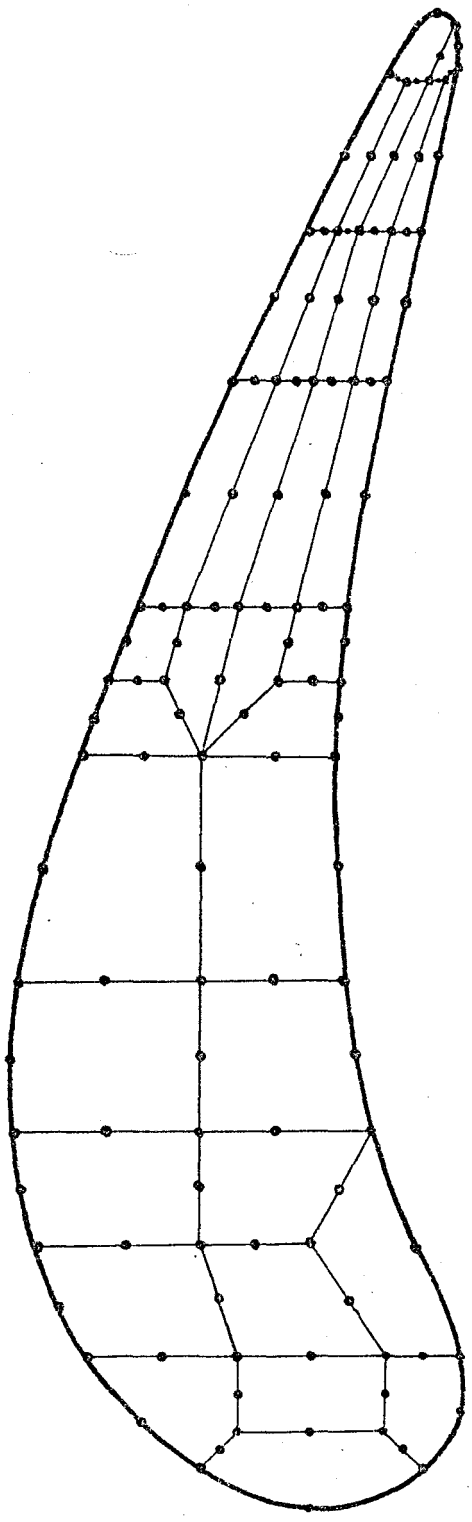

10 mm

l = 60 mm

Z = 0

$D_h = 0$

$D_h / l = 0.00$

FIG.11- Geometry of BLADE-A in discretisized form.

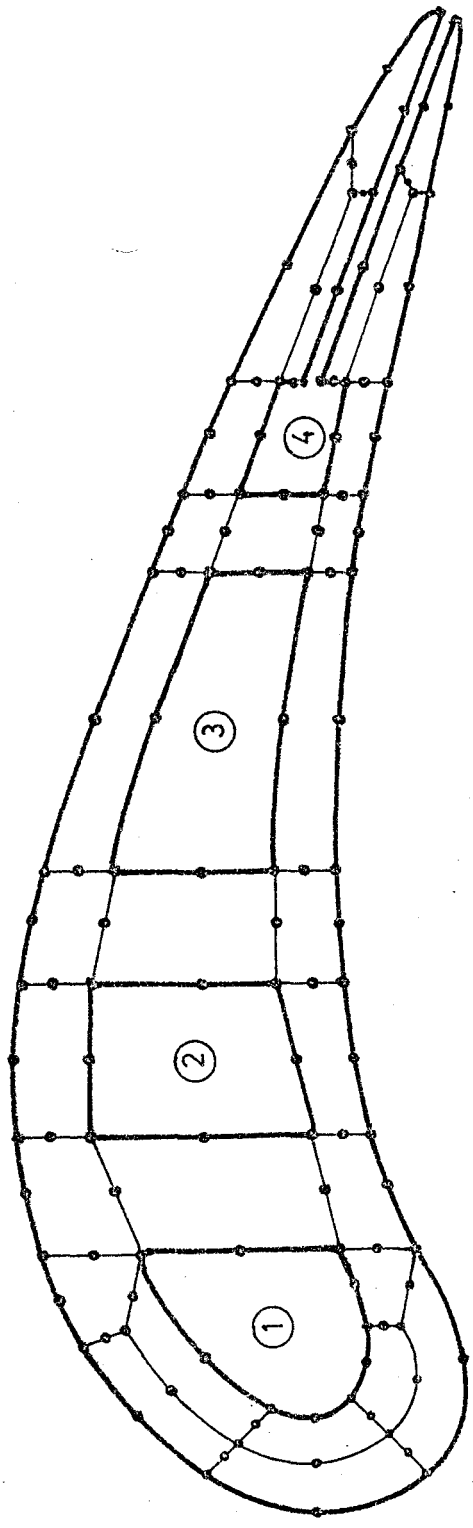

10 mm

l = 60 mm

Z = 120

D_h= 17.40

$D_h / l = 0.29$

FIG.12- The geometry of BLADE-B in discretisized form.

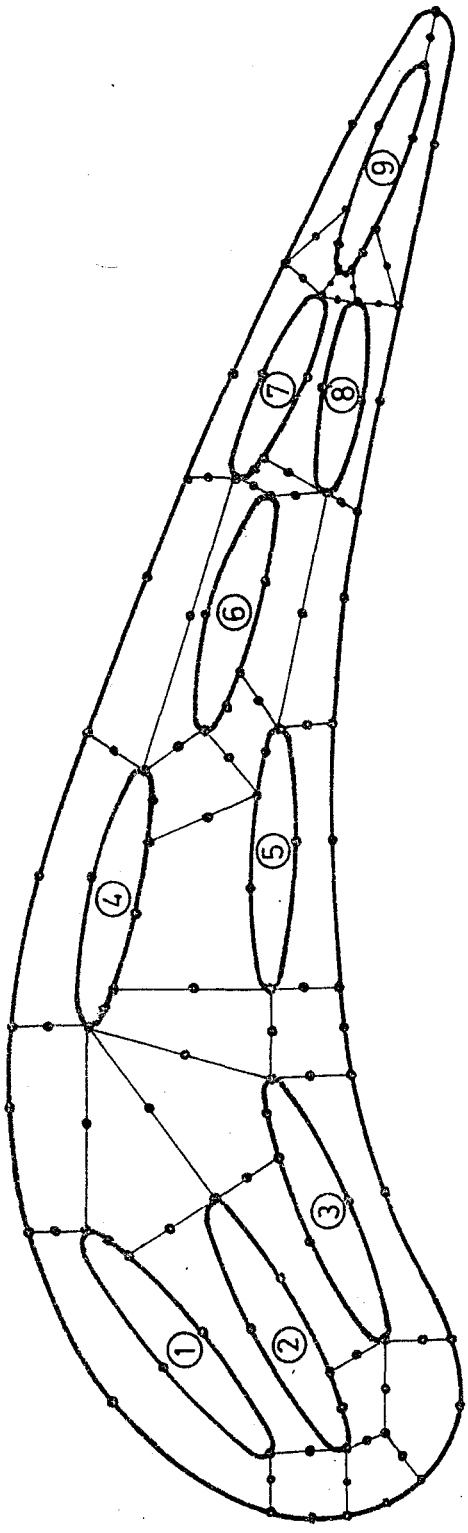

FIG.13- The geometry of BLADE-C in discretisized form.

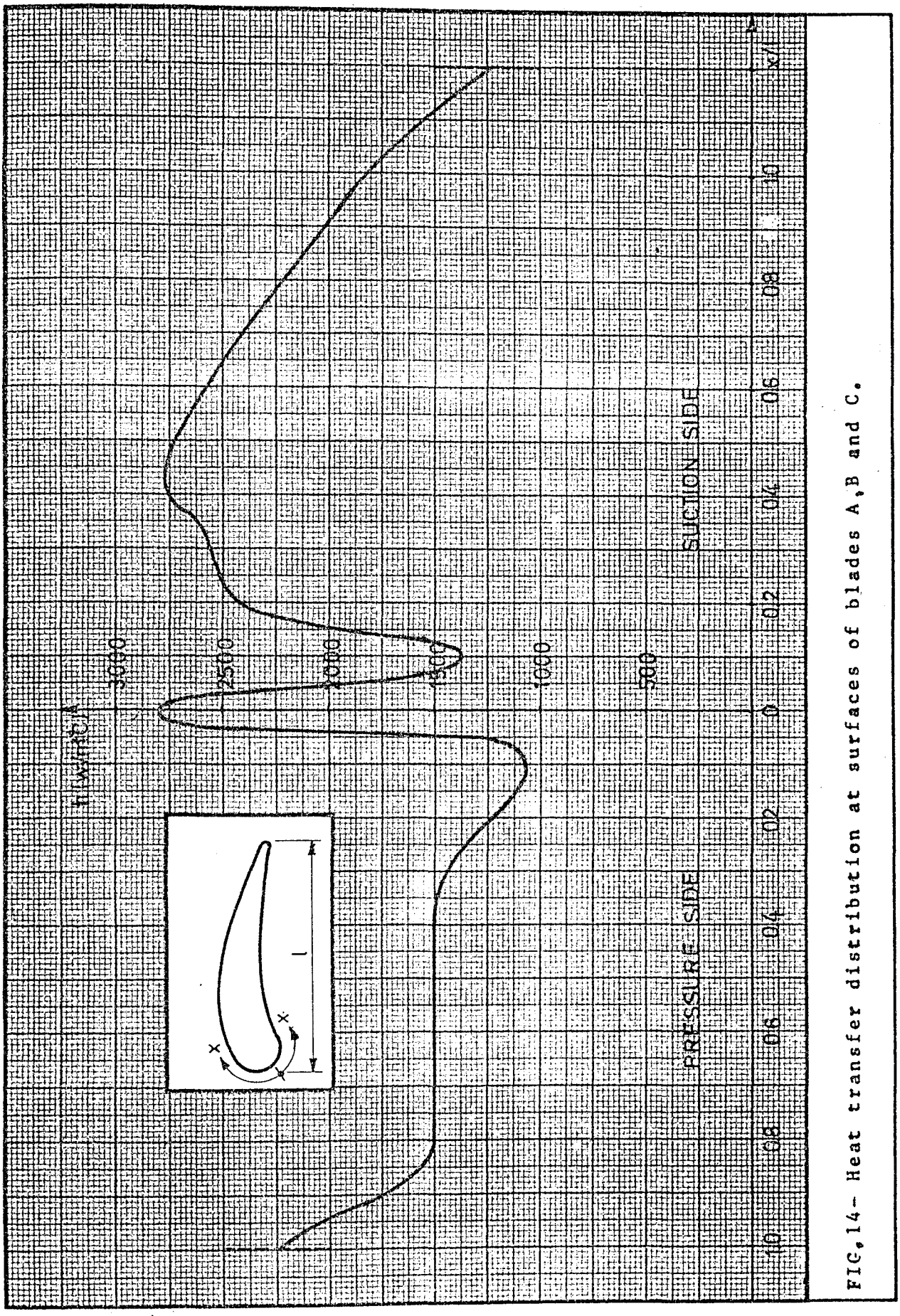

FIG. 14- Heat transfer distribution at surfaces of blades A, B and C.

BLADE-A

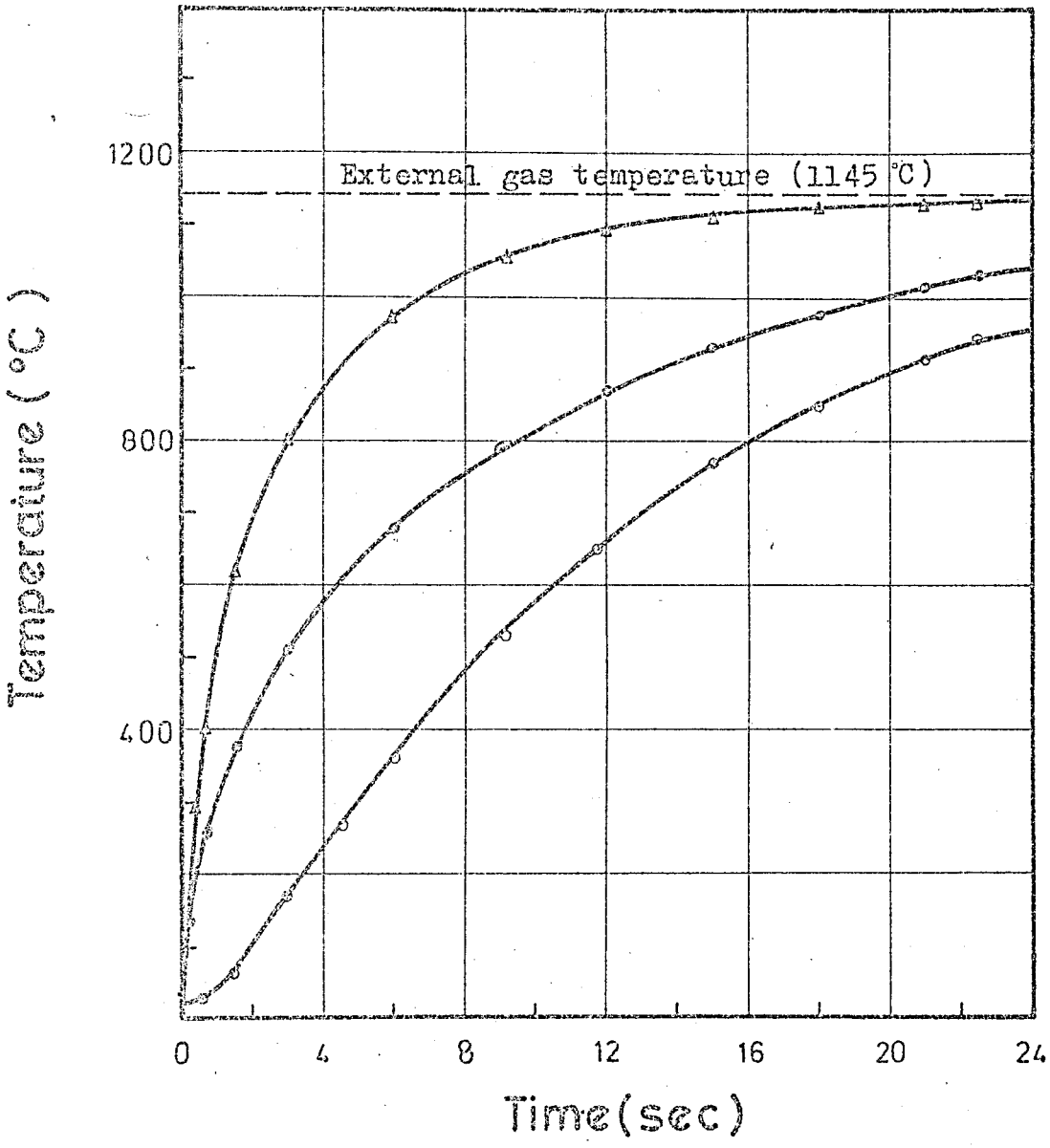

FIG.15- Transient temperature at three locations in BLADE-A.

BLADE-B

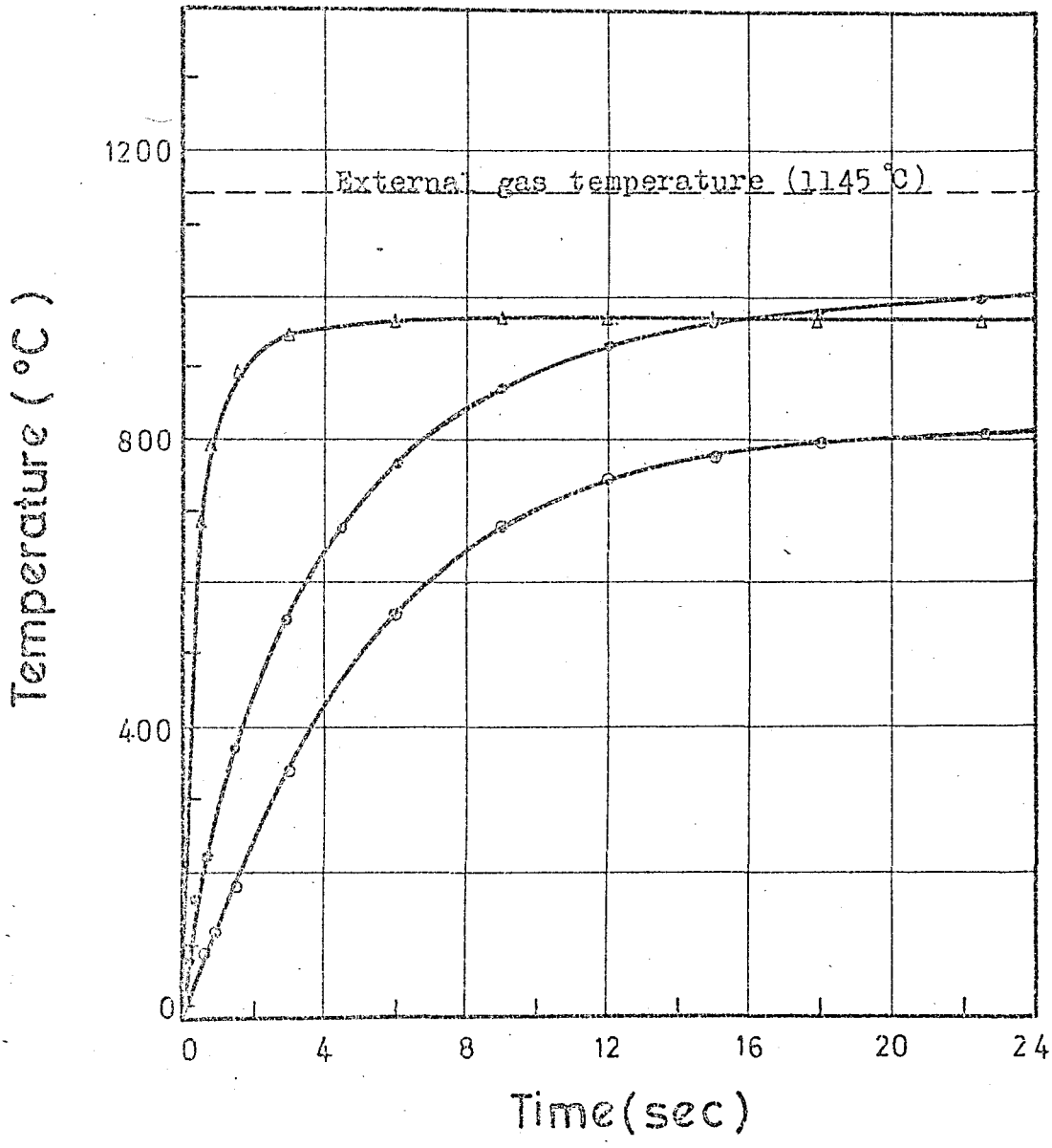

⊙ Stagnation point

○ Mid-point

△ Trailing edge end

FIG.16- Transient temperature at three locations in BLADE-B.

BLADE-C

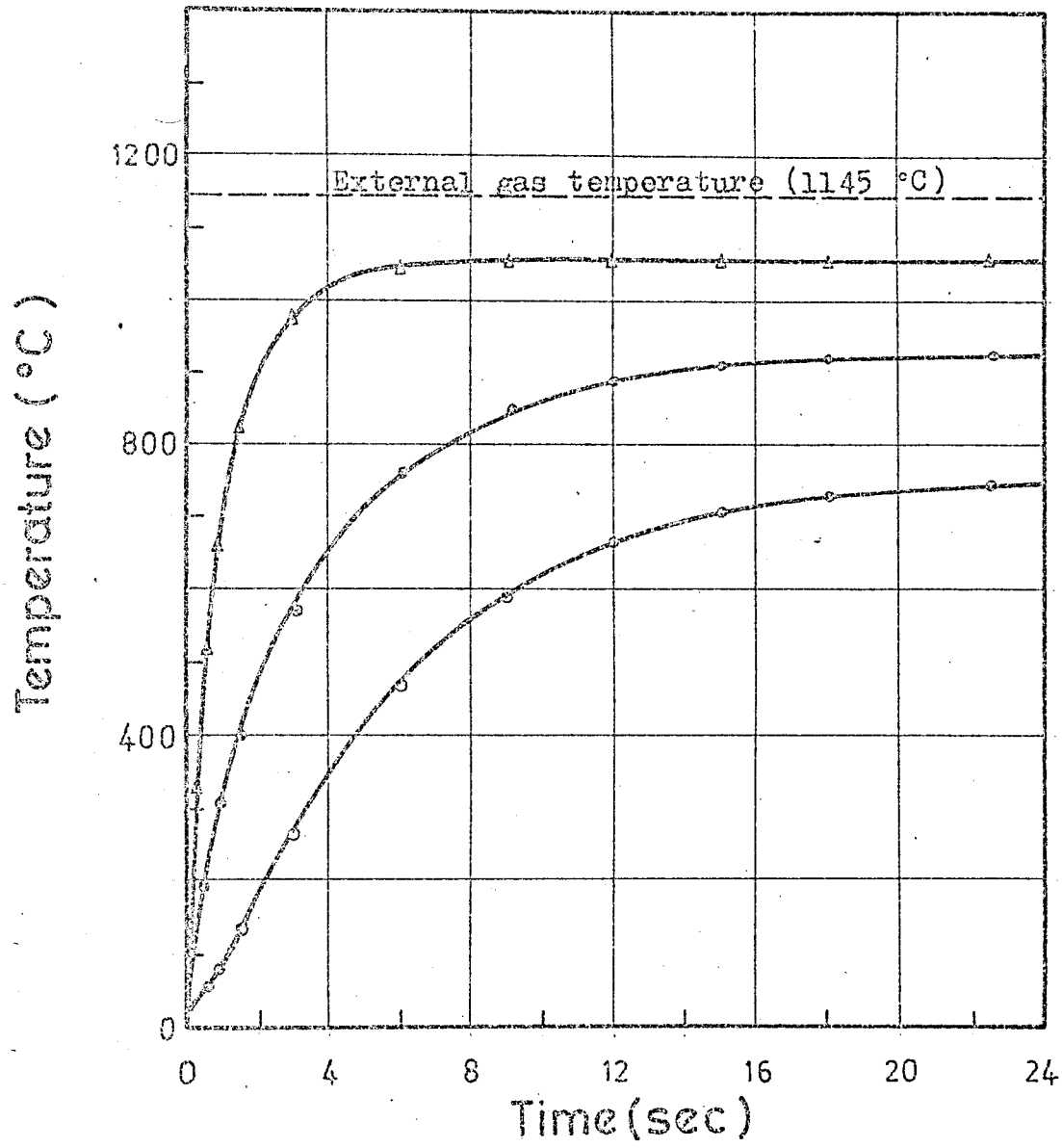

∘ Stagnation point
∘ Mid-point
△ Trailing edge end

FIG.7- Transient temperature at three locations in BLADE-C.

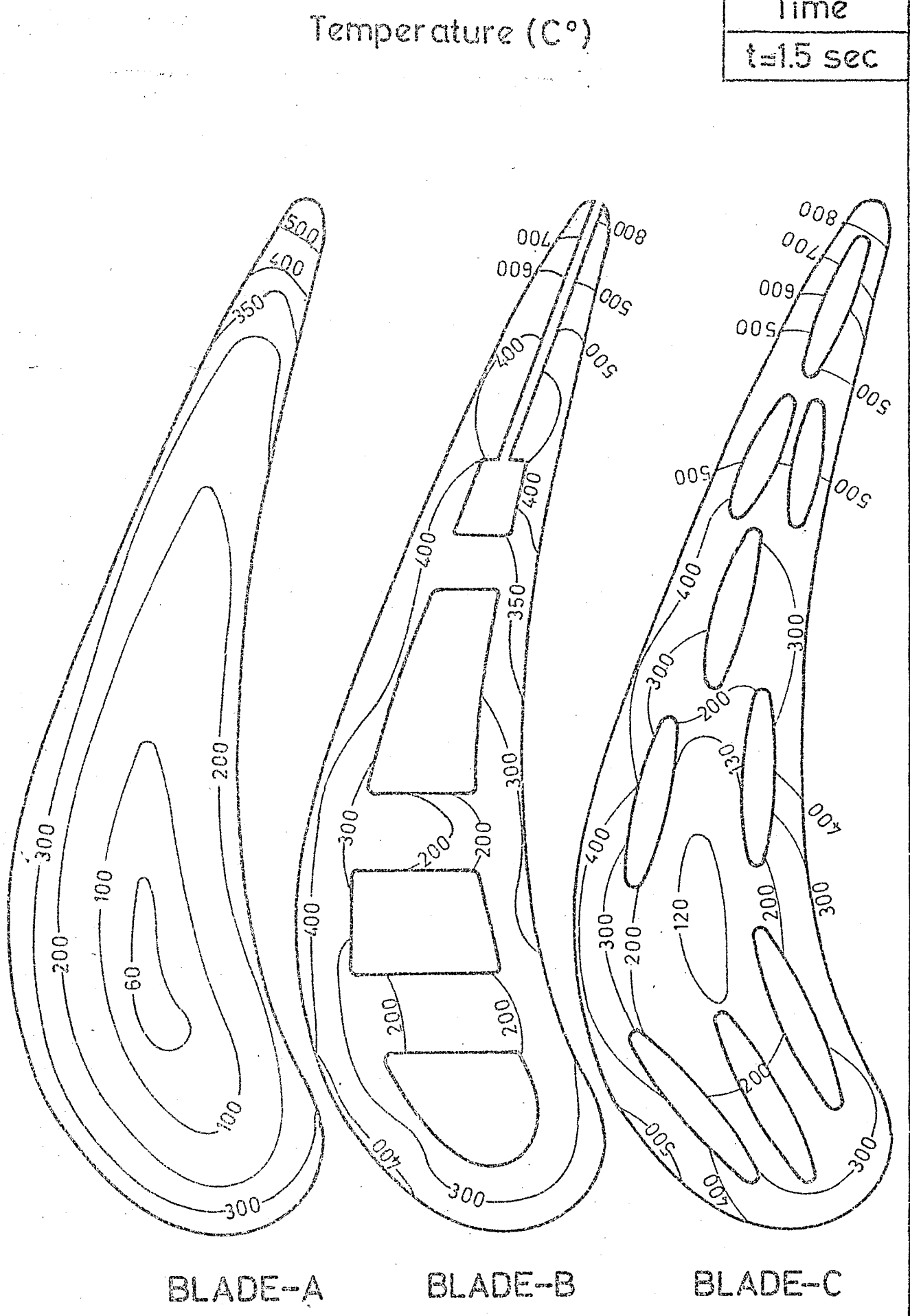

FIG.18- Temperature distributions on blade sections at a time of 1.5 seconds.

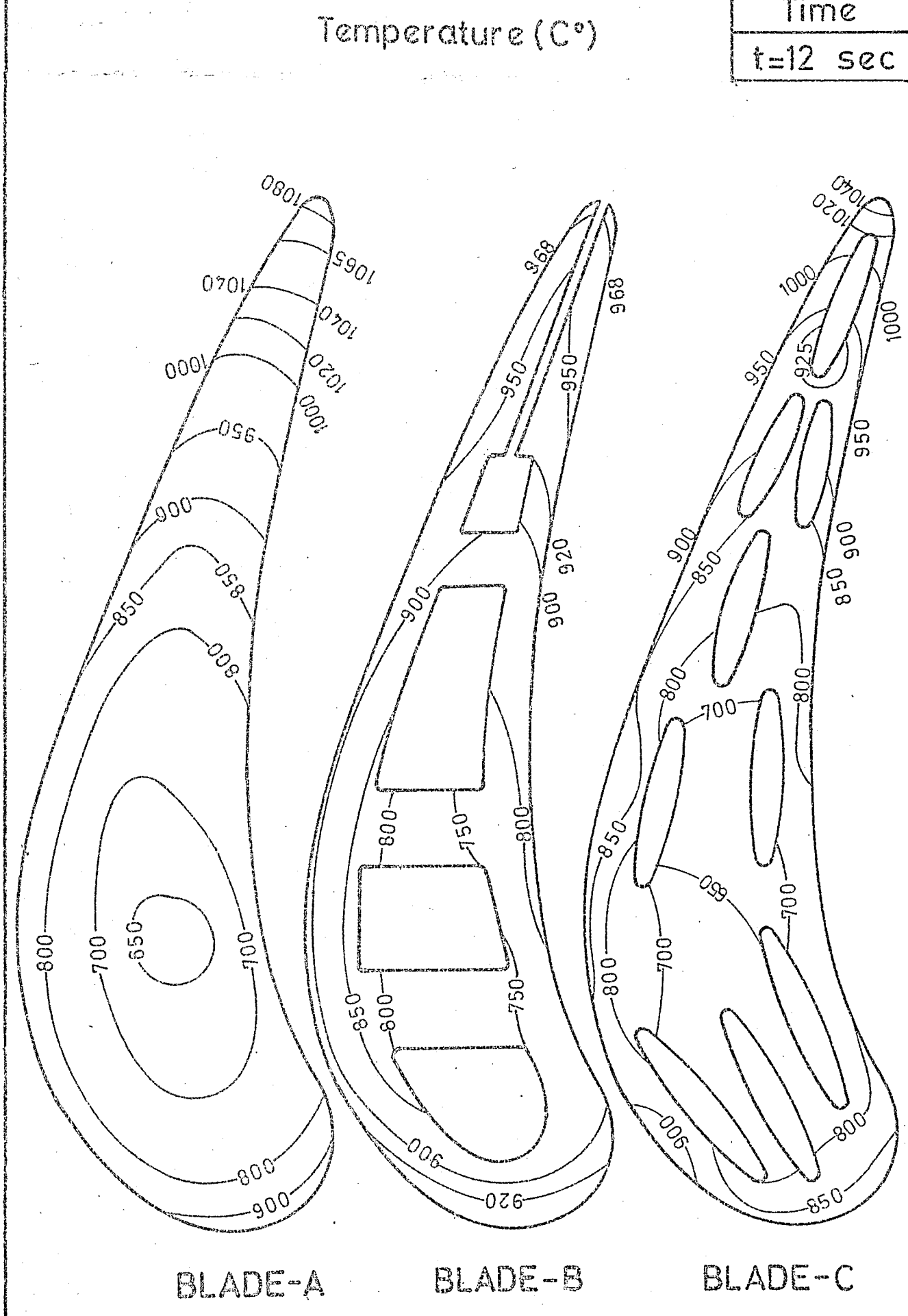

FIG.19- Temperature distributions on blade sections at a time of 12 seconds..

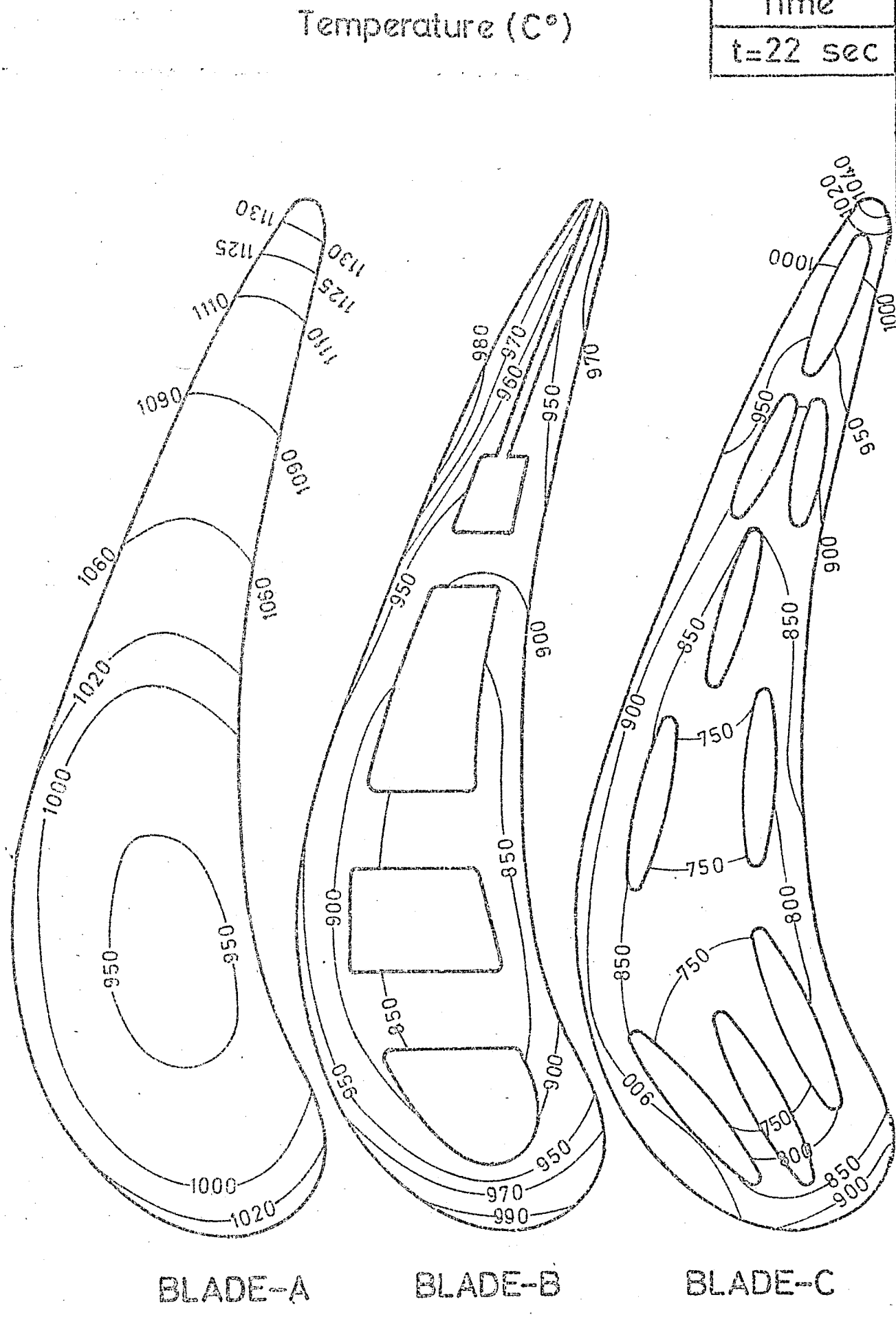

FIG. 20- Temperature distributions on blade sections at a time of 22 seconds.

BLADE-A

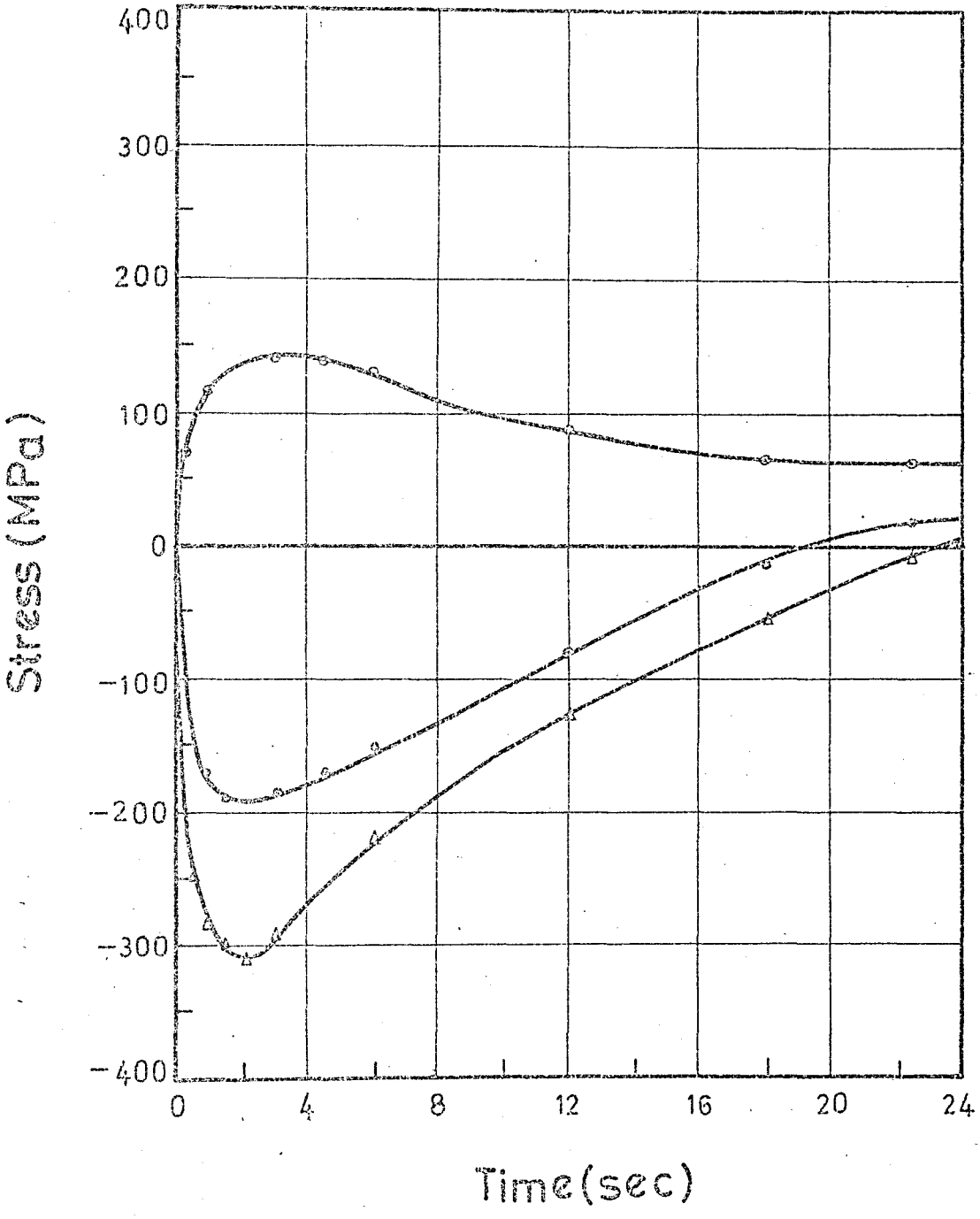

FIG.21- Calculated stress distributions in BLADE-A during start for leading edge, mid-point, and trailing edge

BLADE-B

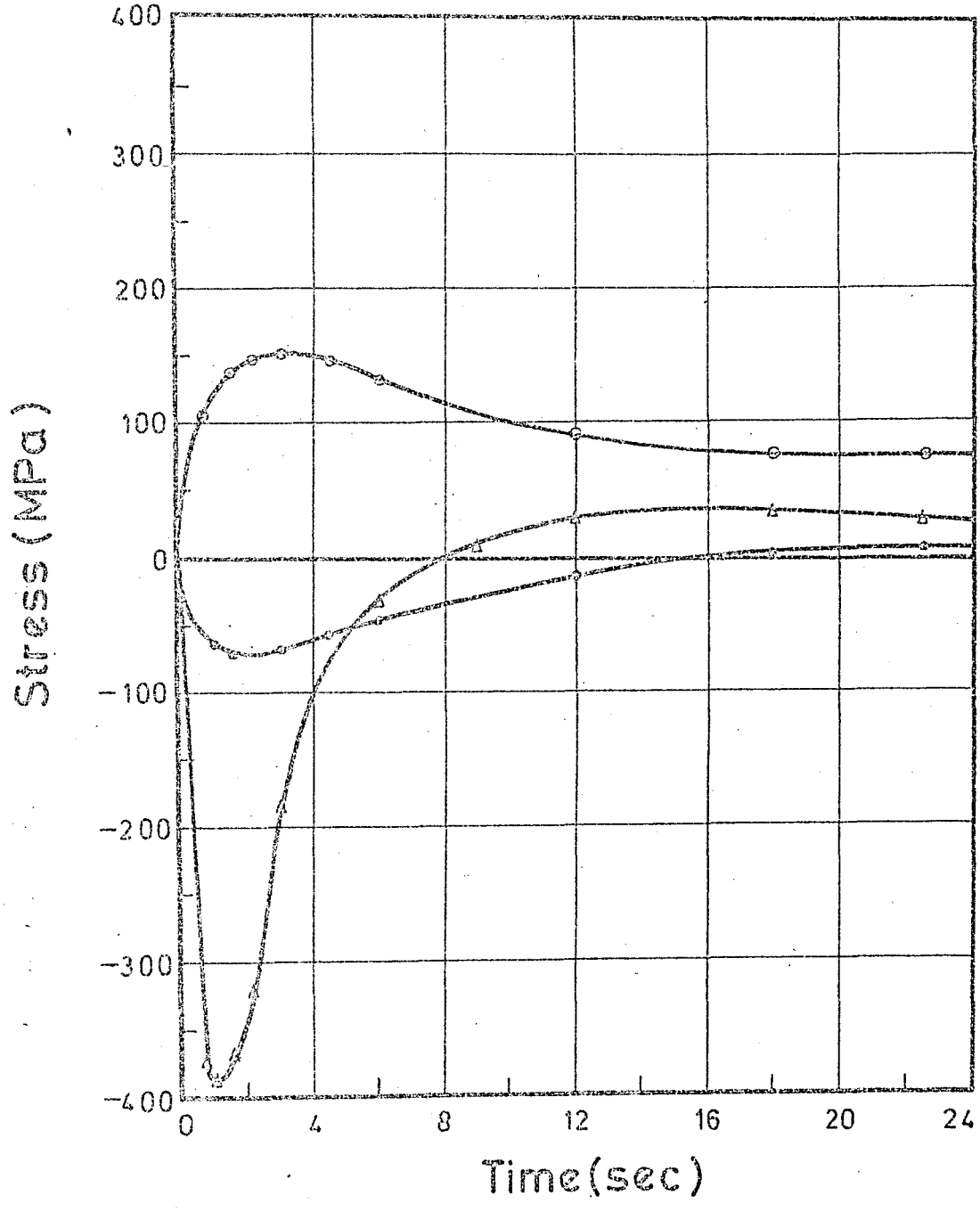

FIG.22-Calculated stress distributions in BLADE-B during start for leading edge, mid-point, and trailing edge

BLADE-C

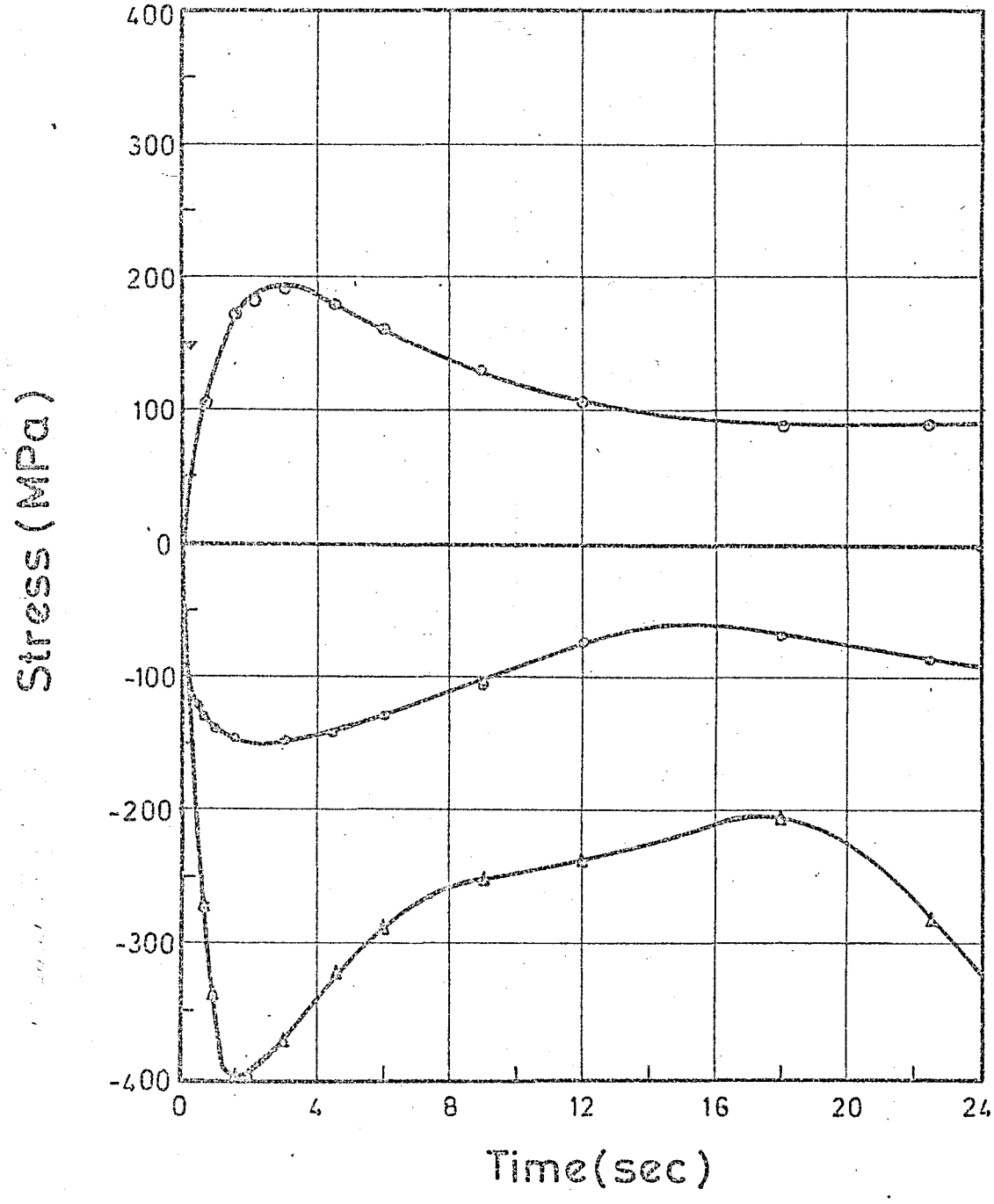

FIG.23- Calculated stress distributions in BLADE-C during start for leading edge, mid-point, and trailing edge.

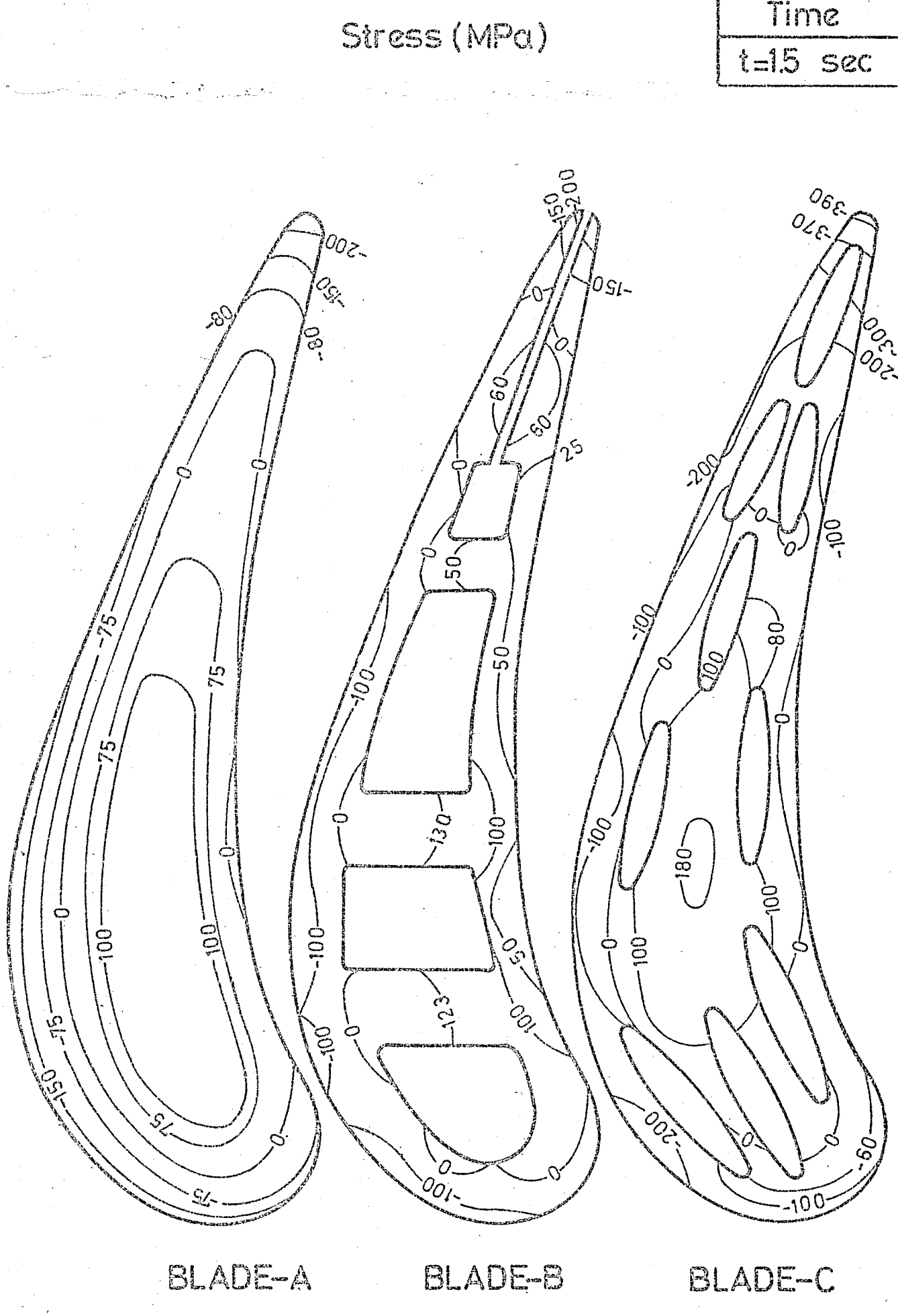

FIG.24- Stress distributions in blade sections at a time of 1.5 sec.

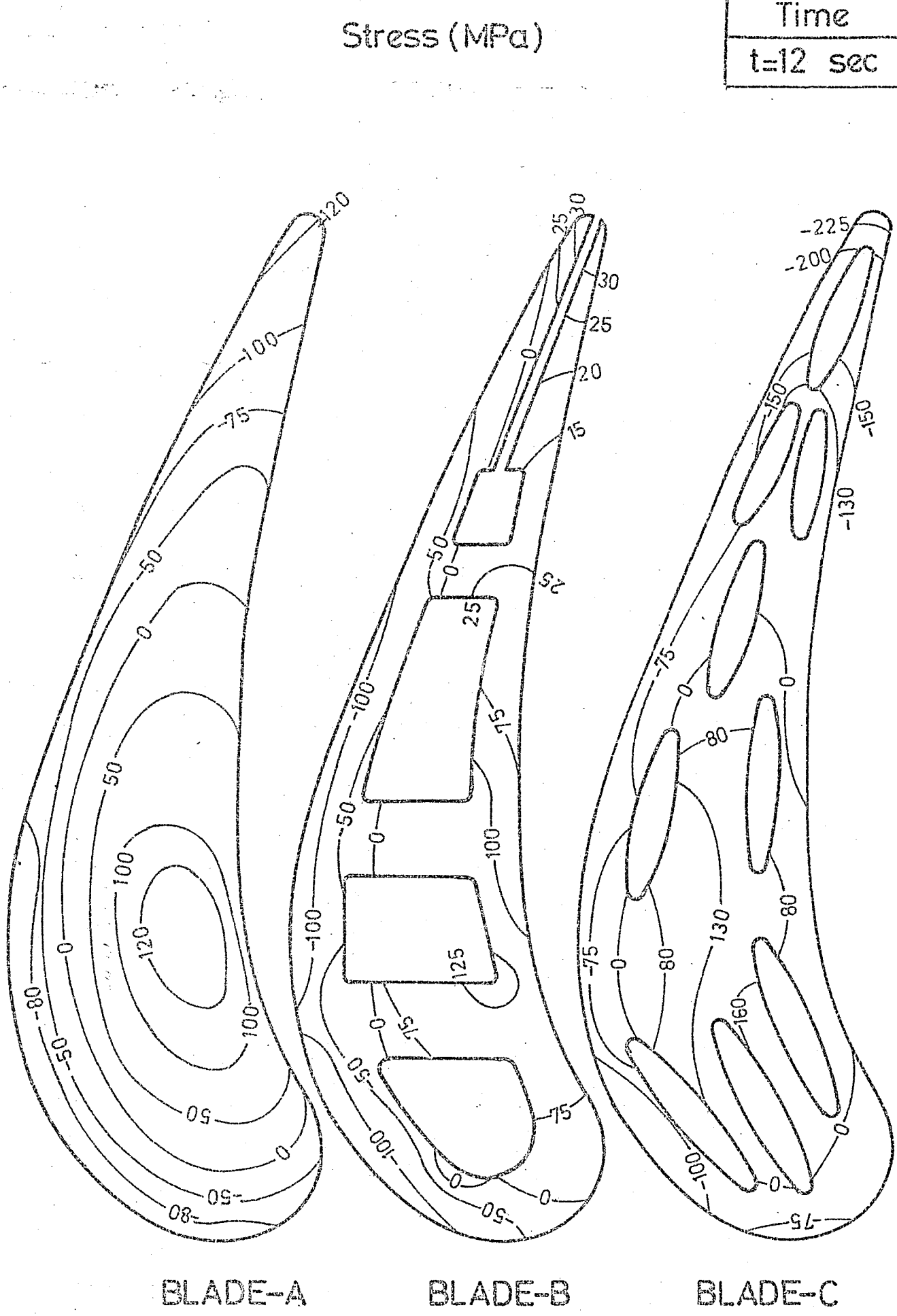

FIG. 25 – Stress distributions in blade sections at time 12 seconds.

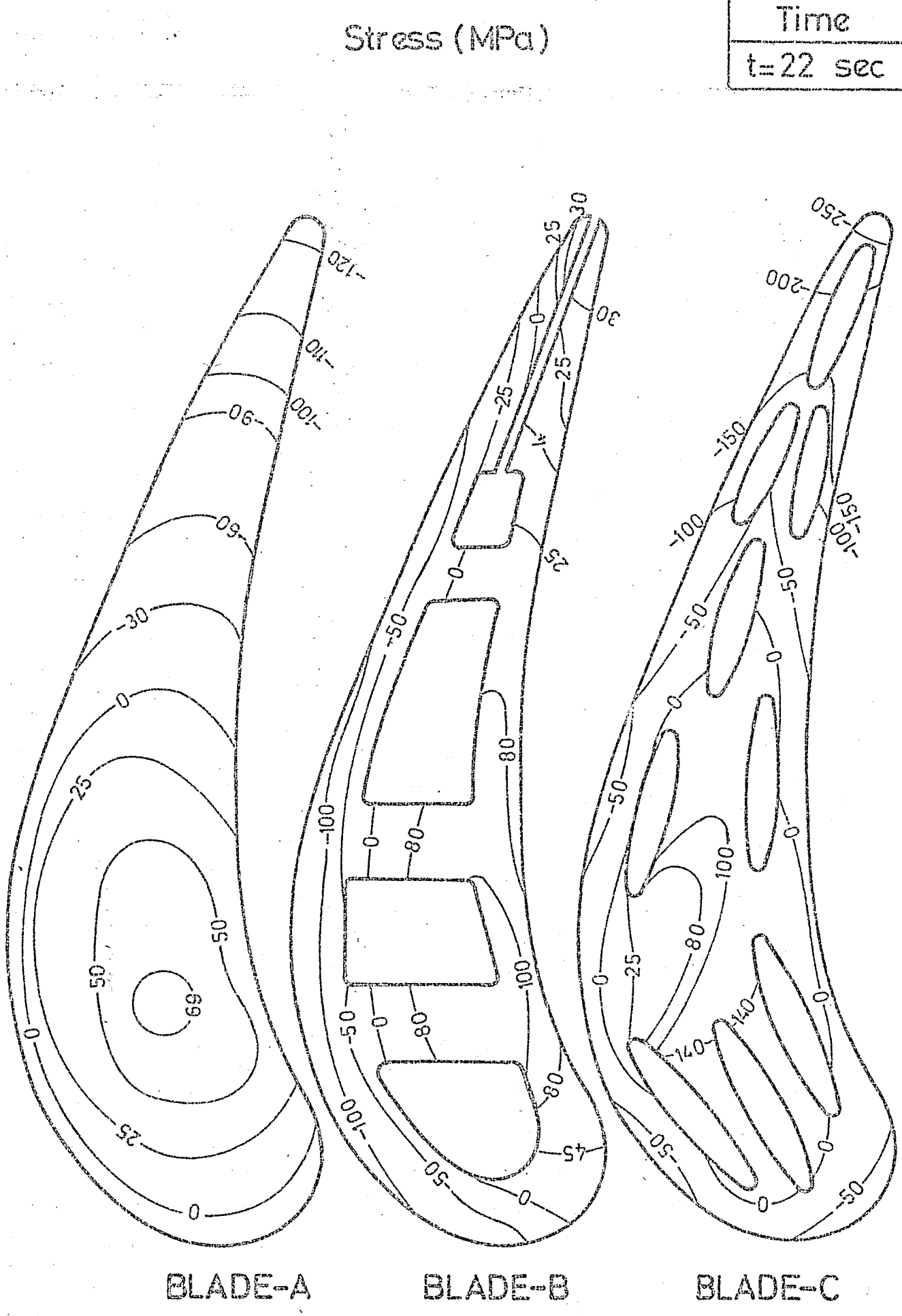

FIG.26- Stress distributions in blade sections at time 22 seconds.

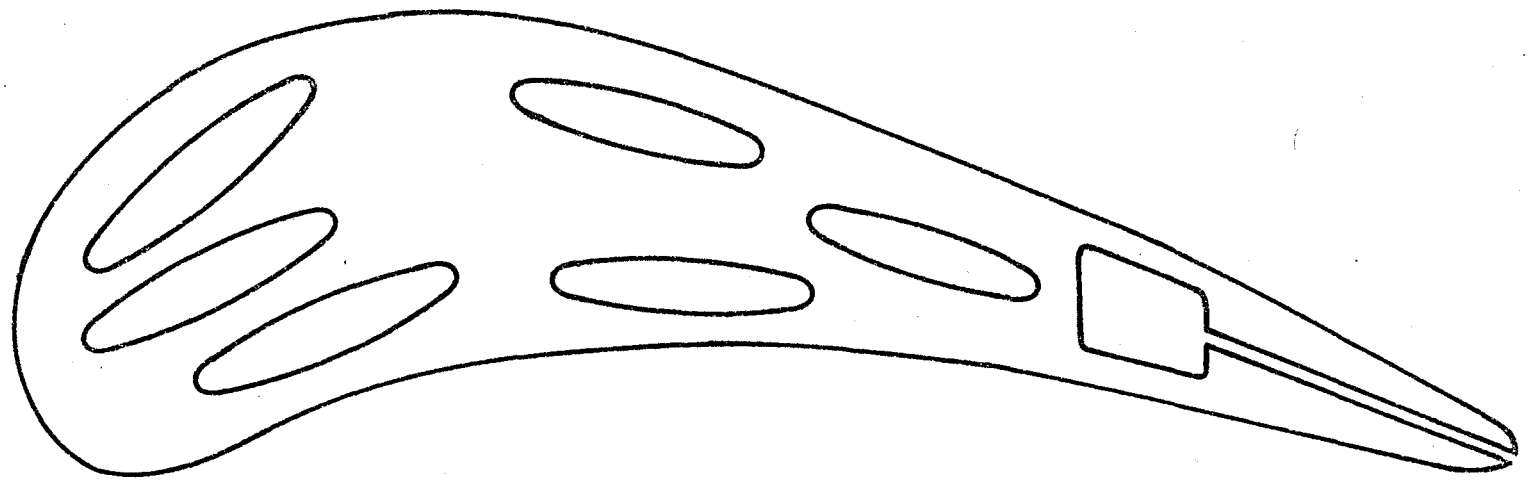

FIG.27- Proposed gas turbine blade for effective cooling geometry and lower thermal stresses.

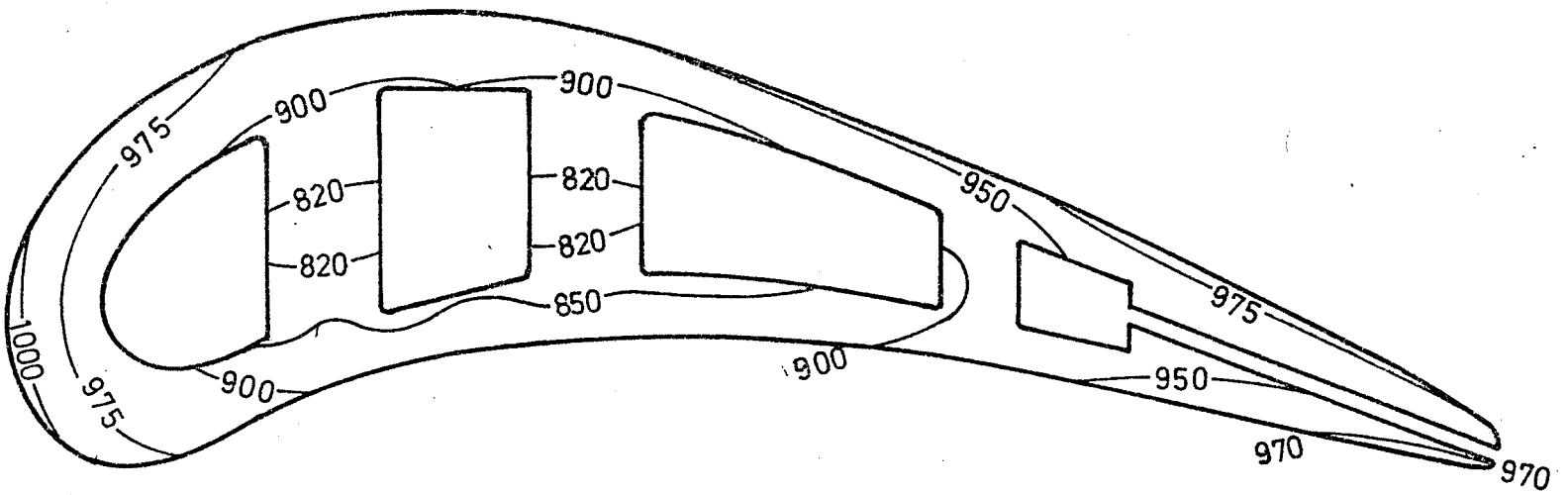

FIG.28- Steady state temperature distribution in BLADE-B_o

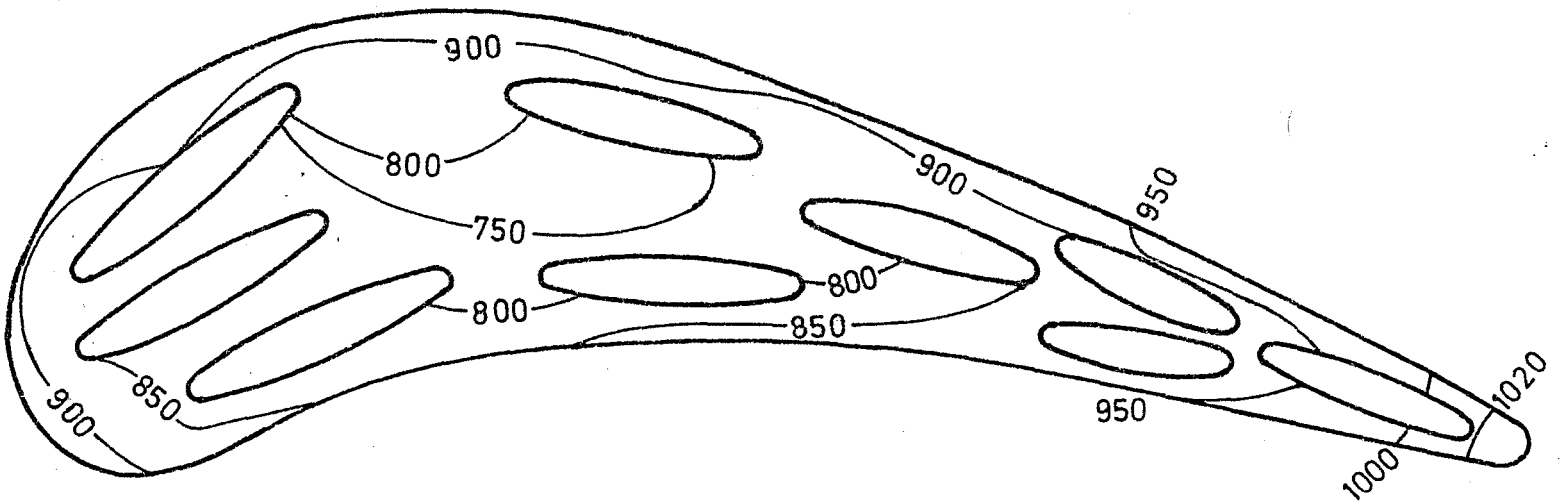

FIG.29- Steady state temperature distributions in BLADE-C.

APPENDIX A

SHAPE FUNCTIONS OF A RECTANGULAR QUADRATIC ELEMENT

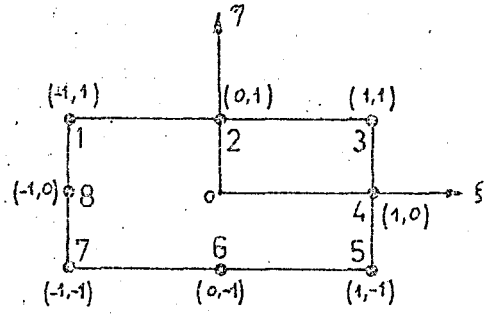

NODE NO.	SHAPE FUNCTIONS
1	$\frac{1}{4}(1-\xi)(1+\eta)(\eta-\xi-1)$
2	$\frac{1}{2}(1-\xi^2)(1+\eta)$
3	$\frac{1}{4}(1+\xi)(1+\eta)(\eta+\xi-1)$
4	$\frac{1}{2}(1+\xi)(1-\eta^2)$
5	$\frac{1}{4}(1+\xi)(1-\eta)(\xi-\eta-1)$
6	$\frac{1}{2}(1-\eta)(1-\xi^2)$
7	$\frac{1}{4}(1-\xi)(1-\eta)(-\eta-\xi-1)$
8	$\frac{1}{2}(1-\xi)(1-\eta^2)$

APPENDIX B

INTEGRATION RESULTS FOR LINE INTEGRALS USED IN THE ANALYSIS

TYPE		INTEGRAL TERMS (INTEGRATION LIMITS : $0 \sim S_3$)	INTEGRATION RESULTS
CONVECTION MATRIX TERMS	(1,1)	$\int N_1^2\, ds = \int \frac{(s-S_2)^2 (s-S_3)^2}{(S_2 S_3)^2}\, ds$	$\frac{(S_3)^3}{30(S_2)^2} - \frac{(S_3)^2}{6 S_2} - \frac{S_3}{3}$
	(1,2)	$\int N_1 N_2\, ds = \int \frac{(s-S_2)(s-S_3)^2 s}{S_3 (S_2)^2 (S_2-S_3)}\, ds$	$\frac{1}{(S_2-S_3)} \left(\frac{(S_3)^4}{30(S_2)^2} - \frac{(S_3)^3}{12 S_2} \right)$
	(1,3)	$\int N_1 N_3\, ds = \int \frac{s(s-S_2)^2 (s-S_3)}{S_2 (S_3)^2 (S_3-S_2)}\, ds$	$\frac{1}{(S_3-S_2)} \left(\frac{(S_3)^3}{20 S_2} - \frac{S_2 S_3}{6} + \frac{S_3^2}{6} \right)$
	(2,1)	$\int N_2 N_1\, ds = \int N_1 N_2\, ds$	
	(2,2)	$\int N_2^2\, ds = \int \frac{(s)^2 (s-S_3)^2}{(S_2)^2 (S_2-S_3)^2}\, ds$	$\frac{(S_3)^5}{30(S_2)^2 (S_2-S_3)^2}$
	(2,3)	$\int N_2 N_3\, ds = \int \frac{-(s)^2 (s-S_3)(s-S_2)}{S_2 S_3 (S_2-S_3)^2}\, ds$	$\frac{1}{(S_2-S_3)^2} \left(\frac{(S_3)^4}{20 S_2} - \frac{(S_3)^3}{12} \right)$
	(3,1)	$\int N_3 N_1\, ds = \int N_1 N_3\, ds$	
	(3,2)	$\int N_3 N_2\, ds = \int N_2 N_3\, ds$	
	(3,3)	$\int N_3^2\, ds = \int \frac{(s)^2 (s-S_2)^2}{(S_3)^2 (S_3-S_2)^2}\, ds$	$\frac{1}{(S_3-S_2)^2} \left(\frac{S_3 (S_2)^2}{3} - \frac{S_2 (S_3)^2}{2} + \frac{(S_3)^3}{5} \right)$
THERMAL FORCE VECTOR TERMS	(1)	$\int N_1\, ds = \int \frac{(s-S_2)(s-S_3)}{S_2 S_3}\, ds$	$\frac{S_3}{2} - \frac{(S_3)^2}{6 S_2}$
	(2)	$\int N_2\, ds = \int \frac{s(s-S_3)}{S_2 (S_2-S_3)}\, ds$	$-\frac{(S_3)^3}{6 S_2 (S_2-S_3)}$
	(3)	$\int N_3\, ds = \int \frac{s(s-S_2)}{S_3 (S_3-S_2)}\, ds$	$\frac{1}{(S_3-S_2)} \left(\frac{(S_3)^2}{3} - \frac{S_3 S_2}{2} \right)$

TABLE 1 : PROPERTIES OF INCONEL 600

DESIGNATION	Max. Recommended Temp.°C	HARDNESS BHN	Elastic Modulus 20°C MPa	UTS 20°C MPa	Density kg/m³	Coeff. Thermal Expansion		Thermal Conductivity Joules/m°C sec		
						300°c m/m°c	650°c m/m°C	20°C	300°C	650°C
Inconel 600	1200	187 Max.	21	550	8442	1.4×10^{-5}	1.5×10^{-5}	15	19	24.8

TABLE 2 : INTERNAL COOLING CONDITIONS

BLADE-B			BLADE-C		
DUCT	T (°C)	h(w/m²°C)	DUCT	T (°C)	h(w/°Cm²)
1	500	0.0248	1-2-3	500	0.0262
2-3	500	0.0265	4-5-6	500	0.0265
4	700	0.0232	7-8-9	700	0.0232

APPENDIX D

COMPUTER PROGRAM : FINEL

The following fortran program is to solve two-dimensional transient heat conduction problem given in Chapter III. The boundary conditions considered in the program are both prescribed temperature (Dirichlet type) and convective heat transfer (Neumann) type of conditions.

DESCRIPTION OF THE COMPUTER CODE

This program is adequate for the meshes with maximum 130 nodes. In the program, the local coordinates of the nodes of elements and weighting factors of integration belonging to these nodes are recorded as data in statements 8-13. In statements 14 and 15 the numbers of elements and nodes, and the number of nodes under prescribed temperature condition are read under names NEL, NNODS and NCT, respectively.

The statements 16-21 are for the loops initializing the global conduction matrix, global capacitance matrix, global thermal force vector and unknown temperature vector by setting all their terms equal to zero.

After reading in the necessary data,calculation of the values of both shape functions and first derivatives of these functions with respect to the local coordinates ξ and η at each node of an element is calculated and stored in the loops between statements 30-67,Calculation of the element matrices and their assemblage into global ones begin with the statement 68 and end with the statement 126,The details of the procedure followed are as below:

1-) Loop 7 and 8 (statements 70-75) : These loops initialize the element conduction matrix and element capacitance matrix by setting their terms equal to zero,

2-) Loop 13 (statements 76-115) : This loop is used to form the Jacobian matrix and element matrices mentioned in step 1,

2,1-) Loop 9 (statements 81-90) : The terms of Jacobian matrix are formed in this step,

2,2-) Loop 11 (statements 100-102) : The terms of element capacitance matrix are calculated in this loop,

2,3-) Loop 12 (statements 103-109) : This loop calculates the terms of element conduction matrix,

2,4-) Loop 13 (statements 111-115) : This loop calculates the terms of element convection matrix,

3-) Loop 15 (statements 120-125) : In this loop,the assemblage of element conduction matrix and element capacitance matrix into global conduction matrix and global capacitance matrix is realized. This part of the program together with section 3,8 of the thesis illustrates the assembly process in finite element method.

The time integration data,the time increment and the number of time increments are read in statement 127 under names DT and NT, Initial condition data,initial temperature values of all nodes, TIN(I) are input in statement 129,By using these data,the governing matrix equation is rearranged and a simpler equation is establised which has the form,

Now,the governing matrix equation is ready to be modified for the boundary conditions Loop 17 is for this purpose and its first statement numbered 137 inputs the boundary condition data.In statements from 143 to 164,the governing equation is modified for the prescribed temperature boundary conditions and in statements from 165 to 212 convective heat transfer boundary conditions are applied to the governing equation.

In solving the system of equations obtained LU decomposition is used,[31] .The statements from 214 to 273 contain the steps of this solution procedure.

The preparation of input data of the problem to be solved by using program FINEL should be made according to the format statements 275-287,The program prints the calculated values of the unknown variable at the end of the program according to an output control data read in statements 236-239.

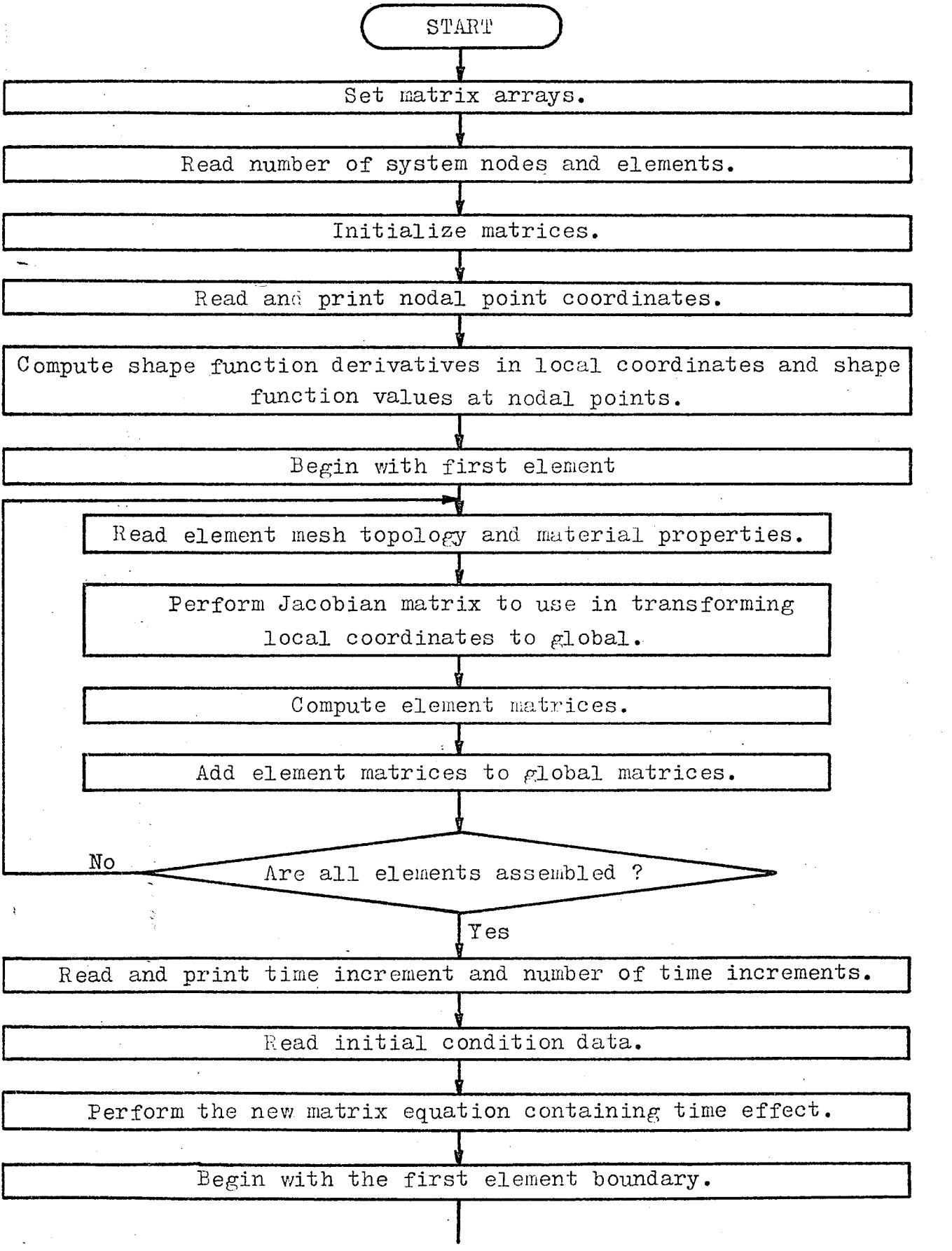

FLOW CHART OF THE PROGRAM "FINEL".

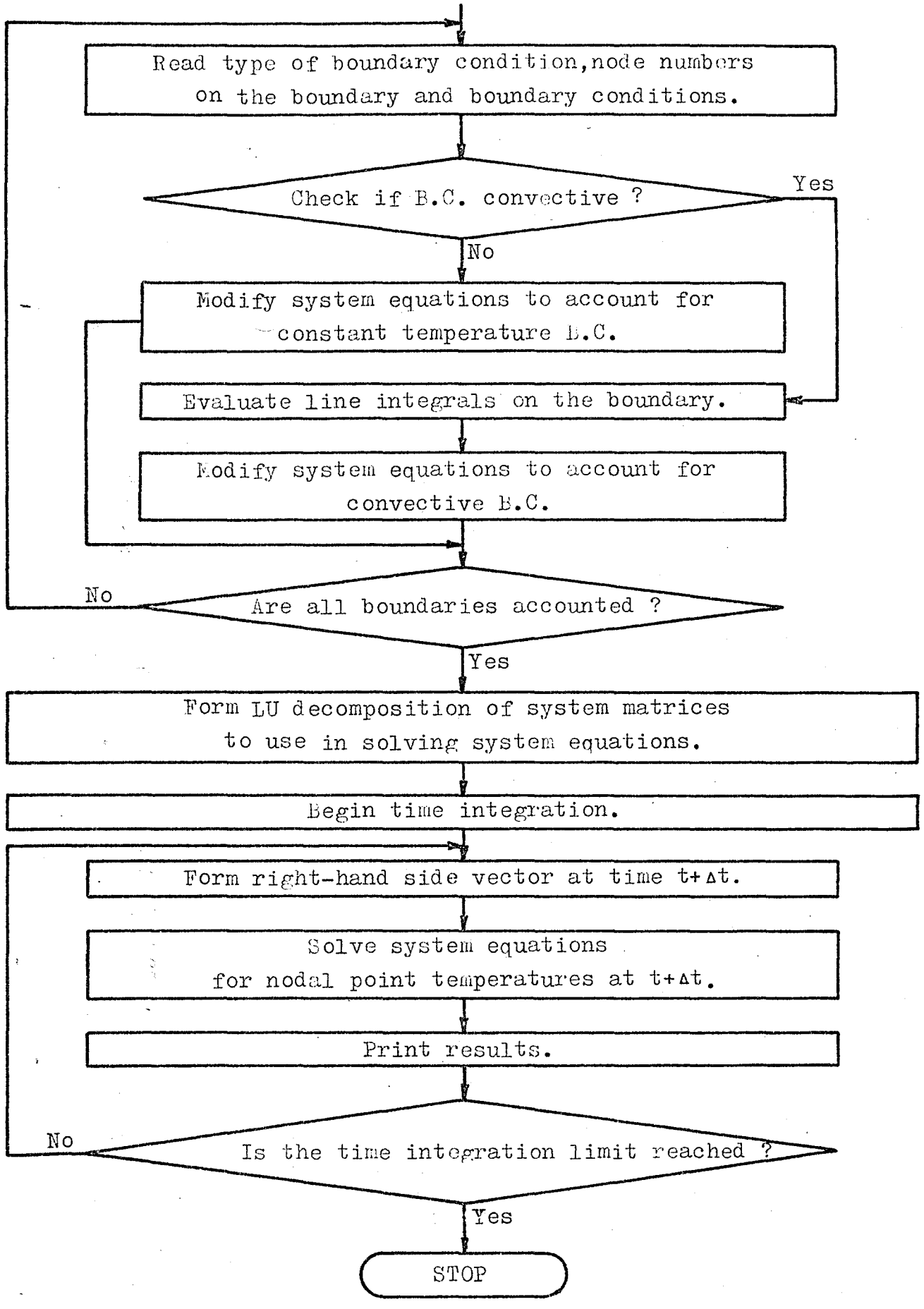
Read type of boundary condition, node numbers on the boundary and boundary conditions.
Check if B.C. convective ?
Yes
No
Modify system equations to account for constant temperature B.C.
Evaluate line integrals on the boundary.
Modify system equations to account for convective B.C.
No
Are all boundaries accounted ?
Yes
Form LU decomposition of system matrices to use in solving system equations.
Begin time integration.
Form right-hand side vector at time t+Δt.
Solve system equations for nodal point temperatures at t+Δt.
Print results.
No
Is the time integration limit reached ?
Yes
STOP

(Continued)

PROGRAM FINEL

```
      REAL JAK1,JAK2,JAK3,JAK4,IJAK1,IJAK2,IJAK3,IJAK4
      DIMENSION WR(9),XLOC(9),YLOC(9),DNXSI(9,8),DNETA(9,8),VALN(9
      DIMENSION CSAB(8,8),AK(8,8),NODS(8),B(2,8),BT(8,2),CX(5),CY(5
      DIMENSION A(130,130),C(130,130),BS(130),T(130),X(130),Y(130)
      DIMENSION S(5),SMAT(3,3),SVEC(3),IGX(3),TINF(3),NOD(3),ISWC(5
      DIMENSION TIN(150),BSAB(150),BSUB(150),KKOD(500),NODT(150)
      DIMENSION YM(130),XM(130)
      DATA XLOC/-1.0,0.0,1.0,1.0,1.0,0.0,-1.0,-1.0,0.0/
      DATA YLOC/-1.0,-1.0,-1.0,0.0,1.0,1.0,1.0,0.0,0.0/
      DATA WR/1.0,4.0,1.0,4.0,1.0,4.0,1.0,4.0,16.0/
      DATA ISWC/0,0,1,0,1/
      DO 1 I=1,9
    1 WR(I)=WR(I)/9.0
      READ(5,101)NEL,NNODS
      READ(5,114)NCT
      DO 2 I=1,NNODS
      BS(I)=0.0
      T(I)=20.
      DO 2 J=1,NNODS
      A(I,J)=0.0
    2 C(I,J)=0.0
      READ(5,102)(X(I),Y(I),I=1,NNODS)
      IF(ISWC(1).EQ.1) GO TO 3
      WRITE(6,103)(X(I),Y(I),I=1,NNODS)
    3 CONTINUE
      DO 4 I=1,NNODS
      X(I)=X(I)/10.
    4 Y(I)=Y(I)/10.
      DO 5 I=1,9
      XSI=XLOC(I)
      ETA=YLOC(I)
      SAB1=1.0-ETA
      SAB2=1.0+ETA
      SAB3=1.0-XSI
      SAB4=1.0+XSI
      SAB5=0.5*ETA
      SAB6=0.25*ETA
      SAB7=0.5*XSI
      SAB8=0.25*XSI
      DNXSI(I,1)=(SAB7+SAB6)*SAB1
      DNXSI(I,2)=-XSI*SAB1
      DNXSI(I,3)=(SAB7-SAB6)*SAB1
      DNXSI(I,4)=0.5-SAB5*ETA
      DNXSI(I,5)=(SAB7+SAB6)*SAB2
      DNXSI(I,6)=-XSI*SAB2
      DNXSI(I,7)=(SAB7-SAB6)*SAB2
      DNXSI(I,8)=-0.5+SAB5*ETA
      DNETA(I,1)=(SAB5+SAB8)*SAB3
      DNETA(I,2)=-0.5+SAB7*XSI
      DNETA(I,3)=(SAB5-SAB8)*SAB4
      DNETA(I,4)=-ETA*SAB4
      DNETA(I,5)=(SAB5+SAB8)*SAB4
      DNETA(I,6)=0.5-SAB7*XSI
      DNETA(I,7)=(SAB5-SAB8)*SAB3
      DNETA(I,8)=-ETA*SAB3
      VALN(I,1)=-SAB1*SAB3*(SAB6+SAB8-0.25)
```

```
      VALN(I,2)=SAB1*(0.5-SAB7*XSI)
      VALN(I,3)=-SAB1*SAB4*(SAB6-SAB8+0.25)
      VALN(I,4)=SAB4*(0.5-SAB5*ETA)
      VALN(I,5)=SAB2*SAB4*(SAB6+SAB8-0.25)
      VALN(I,6)=SAB2*(0.5-SAB7*XSI)
      VALN(I,7)=SAB2*SAB3*(SAB6-SAB8-0.25)
      VALN(I,8)=SAB3*(0.5-SAB5*ETA)
    5 CONTINUE
      IF(ISWC(2).EQ.0) GO TO 6
      WRITE(6,111)((DNXSI(I,J),J=1,8),I=1,9)
    6 CONTINUE
      DO 16 K=1,NEL
      READ(5,104)(NODS(J),J=1,8),COND,ALPHA
      DO 7 I=1,8
      DO 7 J=1,8
    7 CSAB(I,J)=0.0
      DO 8 I=1,8
      DO 8 J=1,8
    8 AK(I,J)=0.0
      DO 13 L=1,9
      JAK1=0.0
      JAK2=0.0
      JAK3=0.0
      JAK4=0.0
      DO 9 M=1,8
      N=NODS(M)
      XVAL=X(N)
      YVAL=Y(N)
      D1=DNXSI(L,M)
      D2=DNETA(L,M)
      JAK1=JAK1+D1*XVAL
      JAK2=JAK2+D1*YVAL
      JAK3=JAK3+D2*XVAL
    9 JAK4=JAK4+D2*YVAL
      DET=JAK1*JAK4-JAK2*JAK3
      IJAK1=JAK4/DET
      IJAK2=-JAK2/DET
      IJAK3=-JAK3/DET
      IJAK4=JAK1/DET
      WRITE(6,106)JAK1,JAK2,JAK3,JAK4,DET
      IF(ISWC(3).EQ.1) GO TO 10
   10 CONTINUE
      CONST=DET*WR(L)*ALPHA
      DO 11 I=1,8
      DO 11 J=1,8
   11 CSAB(I,J)=VALN(L,J)*VALN(L,I)*CONST+CSAB(I,J)
      DO 12 M=1,8
      D1=DNXSI(L,M)
      D2=DNETA(L,M)
      B(1,M)=D1*IJAK1+D2*IJAK2
      B(2,M)=D1*IJAK3+D2*IJAK4
      BT(M,1)=B(1,M)
   12 BT(M,2)=B(2,M)
      CONST=DET*WR(L)*COND
      DO 13 I=1,8
      DO 13 J=1,8
      SUM=BT(I,1)*B(1,J)+BT(I,2)*B(2,J)
      AK(I,J)=AK(I,J)+CONST*SUM
   13 CONTINUE
      IF(ISWC(4).EQ.0) GO TO 14
      WRITE(6,106)((CSAB(I,J),J=1,8),I=1,8)
```

```
      WRITE(6,106)((AK(I,J),J=1,8),I=1,8)
   14 CONTINUE
      DO 15 I=1,8
      L=NODS(I)
      DO 15 J=1,8
      M=NODS(J)
      A(L,M)=A(L,M)+AK(I,J)
   15 C(L,M)=C(L,M)+CSAB(I,J)
   16 CONTINUE
      READ(5,108)DT,NT
      WRITE(6,116)DT,NT
      READ(5,218)(TIN(L),L=1,NNODS)
      DO 23 L=1,NNODS
      DO 23 M=1,NNODS
      CONST=2.0/DT
      ASAB=C(L,M)*CONST+A(L,M)
      C(L,M)=C(L,M)*CONST-A(L,M)
   23 A(L,M)=ASAB
      M=0
   17 READ(5,107)IKOD,NOD1,NOD2,NOD3,TINF1,TINF2,TINF3,H
      TINF(1)=TINF1
      TINF(2)=TINF2
      TINF(3)=TINF3
      IF(IKOD.EQ.0) GO TO 22
      IF(IKOD.EQ.2) GO TO 119
      M=M+1
      MI=M+1
      MJ=M+2
      NODT(M)=NOD1
      NODT(MI)=NOD2
      NODT(MJ)=NOD3
      NOD(1)=NOD1
      NOD(2)=NOD2
      NOD(3)=NOD3
      IJ=3
      IF(IKOD.NE.1) GO TO 19
      IJ=2
   19 CONTINUE
      DO 118 J=1,IJ
      DO 18 I=1,NNODS
      NODE=NOD(J)
      BS(I)=BS(I)-A(I,NODE)*TINF(J)
      A(I,NODE)=0.0
   18 A(NODE,I)=0.0
      A(NODE,NODE)=1.0
  118 BSUB(NODE)=TINF(J)
      GO TO 17
  119 CONTINUE
      CX(1)=X(NOD1)
      CX(3)=X(NOD2)
      CX(5)=X(NOD3)
      CX(2)=0.375*CX(1)+0.75*CX(3)-0.125*CX(5)
      CX(4)=-0.125*CX(1)+0.75*CX(3)+0.375*CX(5)
      CY(1)=Y(NOD1)
      CY(3)=Y(NOD2)
      CY(5)=Y(NOD3)
      CY(2)=0.375*CY(1)+0.75*CY(3)-0.125*CY(5)
      CY(4)=-0.125*CY(1)+0.75*CY(3)+0.375*CY(5)
      S(1)=0.0
      SSUM=0.0
      DO 20 J=1,4
```

```
      I=J+1
      AL1=CX(I)-CX(J)
      AL2=CY(I)-CY(J)
      SSUM=SSUM+SQRT(AL1**2+AL2**2)
   20 S(I)=SSUM
      SA=S(3)
      SB=S(5)
      SA2=SA*SA
      SB2=SB*SB
      SB3=SB2*SB
      SAMB=SA-SB
      SMAT(1,1)=SB3/(30.0*SA2)-SB2/(6.0*SA)+SB/3.0
      SMAT(1,2)=(SB3*SB/(30.0*SA2)-SB3/(12.0*SA))/SAMB
      SMAT(1,3)=(SB3/(20.0*SA)-SB2/6.0+SA*SB/6.0)/SAMB
      SMAT(2,1)=SMAT(1,2)
      SMAT(3,1)=SMAT(1,3)
      SMAT(2,2)=SB3*SB2/(30.0*SA2*SAMB*SAMB)
      SMAT(2,3)=(SB3*SB/(20.0*SA)-SB3/12.0)/(SAMB**2)
      SMAT(3,2)=SMAT(2,3)
      SMAT(3,3)=(SB3/5.0-SA*SB2/2.0+SA2*SB/3.0)/(SAMB**2)
      SVEC(1)=SB/2.0-SB2/(6.0*SA)
      SVEC(2)=-SB3/(6.0*SA*SAMB)
      SVEC(3)=(SA*SB*0.5-SB2/3.0)/SAMB
      IGX(1)=NOD1
      IGX(2)=NOD2
      IGX(3)=NOD3
      DO 21 I=1,3
      IG=IGX(I)
      BS(IG)=BS(IG)+H*TINF(I)*SVEC(I)
      DO 21 J=1,3
      JG=IGX(J)
      C(IG,JG)=C(IG,JG)+H*SMAT(I,J)
   21 A(IG,JG)=A(IG,JG)+H*SMAT(I,J)
      GO TO 17
   22 CONTINUE
      N=NNODS
      N1=N-1
      DO 430 IJ=2,N
  430 A(IJ,1)=A(IJ,1)/A(1,1)
      DO 320 K=2,N1
      NARA=K-1
      NBAS=K+1
      DO 330 J=K,N
      TOPSAT=0.0
      DO 340 IP=1,NARA
  340 TOPSAT=TOPSAT+A(K,IP)*A(IP,J)
  330 A(K,J)=A(K,J)-TOPSAT
      DO 350 I=NBAS,N
      TOPKOL=0.0
      DO 360 IP=1,NARA
  360 TOPKOL=TOPKOL+A(I,IP)*A(IP,K)
  350 A(I,K)=(A(I,K)-TOPKOL)/A(K,K)
  320 CONTINUE
      TOPLAM=0.0
      DO 420 II=1,N1
  420 TOPLAM=TOPLAM+A(N,II)*A(II,N)
      A(N,N)=A(N,N)-TOPLAM
      DO 301 I=1,NT
  301 KKOD(I)=0
      DO 302 J=1,NT,5
  302 KKOD(J)=1
```

```
      DO 30 KK=1,NT
      DO 124 L=1,NNODS
      BSUM=0.0
      DO 24 M=1,NNODS
   24 BSUM=C(L,M)*TIN(M)+BSUM
  124 BSAB(L)=BSUM*2.0*BS(L)
      IF(NCT.EQ.0) GO TO 225
      DO 125 I=1,NCT
      J=NODT(I)
  125 BSAB(J)=BSUB(J)
  225 CONTINUE
      NIT=0
      YM(1)=BSAB(1)
      DO 372 I=2,N
      TOPAL=0.0
      IE1=I-1
      DO 374 K=1,IE1
  374 TOPAL=TOPAL+A(I,K)*YM(K)
  372 YM(I)=BSAB(I)-TOPAL
      XM(N)=YM(N)/A(N,N)
      DO 380 I=2,N
      TOPAL=0.0
      J=N-I+1
      IBAS=J+1
      DO 382 K=IBAS,N
  382 TOPAL=TOPAL+A(J,K)*XM(K)
  380 XM(J)=(YM(J)-TOPAL)/A(J,J)
      DO 29 J=1,NNODS
   29 TIN(J)=XM(J)
      IF(KKOD(KK).EQ.0) GO TO 128
      WRITE(6,109)NIT
      WRITE(6,110)(TIN(J),J=1,NNODS)
  128 CONTINUE
   30 CONTINUE
      WRITE(6,110)(TIN(J),J=1,NNODS)
  101 FORMAT(2I4)
  102 FORMAT(18F4.1)
  103 FORMAT(///,3(7(F6.1,2X,F6.1,2X),/))
  104 FORMAT(8I3,2F10.6)
  106 FORMAT(10X,8F12.6)
  107 FORMAT(I2,3I3,F7.1,2F6.1,F6.4)
  108 FORMAT(F4.2,I3)
  109 FORMAT(///,10X,24H NUMBER OF ITERATIONS : ,I4,/)
  110 FORMAT(1H,10X,3(7(E12.5,2X),/))
  111 FORMAT(///,(/,10X,9F10.3))
  114 FORMAT(I3)
  116 FORMAT(1H1,10X,'TIME INCREMENT = ',F4.2//11X,'TOTAL TIME = ',
  218 FORMAT(16F4.1)
      IF(ISWC(5).EQ.1) GO TO 100
  100 STOP
      END
```